European Journal of Cell Biology 92 (2013) 264–279

Contents lists available at ScienceDirect

European Journal of Cell Biology

journal homepage: www.elsevier.com/locate/ejcb

Neurotrophic factor NT-3 displays a non-canonical cell guidance signaling function for cephalic neural crest cells

Juan P. Zanin, N. Laura Battiato, Roberto A. Rovasio*

Center for Cellular and Molecular Biology – IIBYT (CONICET, UNC), FCEFN, National University of Cordoba, Av. Vélez Sarsfield 1611, 5016 Córdoba, Argentina

ARTICLE INFO

Article history:
Received 22 July 2013
Received in revised form 8 October 2013
Accepted 13 October 2013

Keywords:
Avian embryo
Cell guidance
Cell migration
Chemotaxis
Ciliary ganglion
Electroporation
In situ hybridization
Neural crest cells
Neurotrophic factor-3

ABSTRACT

Chemotactic cell migration is triggered by extracellular concentration gradients of molecules segregated by target fields. Neural crest cells (NCCs), paradigmatic as an accurately moving cell population, undergo wide dispersion along multiple pathways, invading with precision defined sites of the embryo to differentiate into many derivatives. This report addresses the involvement of NT-3 in early colonization by cephalic NCCs invading the optic vesicle region. The results of in vitro and in vivo approaches showed that NCCs migrate directionally up an NT-3 concentration gradient. We also demonstrated the expression of NT-3 in the ocular region as well as their functional TrkB, TrkC and p75 receptors on cephalic NCCs. On whole-mount embryo, a perturbed distribution of NCCs colonizing the optic vesicle target field was shown after morpholino cancelation of cephalic NT-3 or TrkC receptor on NCCs, as well as in situ blocking of TrkC receptor of mesencephalic NCCs by specific antibody released from inserted microbeads. The present results strongly suggest that, among other complementary cell guidance factor(s), the chemotactic response of NCCs toward the ocular region NT-3 gradient is essential for spatiotemporal cell orientation, amplifying the functional scope of this neurotrophic factor as a molecular guide for the embryo cells, besides its well-known canonical functions.

Introduction

Growing evidence of cell communication at a distance has enabled the re-discovery of chemotactic phenomena (Rovasio et al., 2012). This molecular modulation of cell orientation is triggered by extracellular concentration gradients of soluble factors segregated by "target" fields, which are well known in motile bacteria (Chen et al., 2003), amoebas (van Haastert et al., 2007), leukocytes (Gómez-Moutón et al., 2004), neurons (Paratcha et al., 2006), and axonal growth cones (Mortimer et al., 2008). In our laboratory, we have shown chemotaxis of mammal sperm toward the ovular region (Fabro et al., 2002; Giojalas and Rovasio, 1998; Sun et al., 2003), with progesterone signals being the attractant (Guidobaldi et al., 2008; Teves et al., 2006; full references in Guidobaldi et al., 2012). Curiously, the embryonic cell, an accurately distributed cell type, has been less studied from a chemotactic point of view, except in a few documented systems in Drosophila (Molyneaux and Wylie, 2004; Ricardo and Lehmann, 2009), zebrafish (Breau et al., 2012; Molyneaux and Wylie, 2004; Streichan et al., 2011), amphibians (Mayor and Theveneau, 2013), mouse (Belmadani et al., 2005; Kubota and Ito, 2000; Molyneaux and Wylie, 2004; Natarajan et al., 2002; Young et al., 2004) and avian embryos (Kasemeier-Kulesa et al., 2010; McLennan et al., 2012; Rovasio et al., 2012).

The embryonic population of multipotent neural crest cells (NCCs) segregates from the closing neural tube, migrates along defined pathways and colonizes precise sites of the embryo, giving rise to a variety of derivatives, such as neurons, glia, cartilage and pigment cells (Le Douarin and Kalcheim, 1999). Cell behaviors involved in these morphogenetic mechanisms are multiple, complex and clearly modulated by a balance between signals from the genetic background and those present in the near extracellular milieu (Kee et al., 2007; Krispin et al., 2010; Kulesa et al., 2010; Lock et al., 2008; Sauka-Spengler and Bronner-Fraser, 2008). Growing evidence indicates that the migratory competence of NCCs depends on molecules of their micro-environment (Kulesa et al., 2010; Lock et al., 2008; Matthews et al., 2008; Rovasio et al., 1983; Teddy and Kulesa, 2004; Wehrle-Haller et al., 2001). However, these factors are not sufficient to fully explain the oriented migration of this cell population.

Recently, we presented direct evidence of the influence of embryo skin diffusible molecules and Stem Cell Factor (SCF) in eliciting chemotactic oriented migration of cephalic NCCs, also confirming and extending their responsive growth, proliferation and melanocyte differentiation (Rovasio et al., 2012). Those results suggest that SCF may serve as a specific chemoattractant for in vivo guidance of NCCs toward the skin, maintaining its canonic growth

* Corresponding author. Tel.: +54 351 433 2097; fax: +54 351 433 2097.
E-mail address: rrovasio@efn.uncor.edu (R.A. Rovasio).

0171-9335/$ – see front matter © 2013 Elsevier GmbH. All rights reserved.
http://dx.doi.org/10.1016/j.ejcb.2013.10.006

factor activity. Our laboratory also recently showed the CXCR4-dependent chemotactic behavior of cephalic NCCs up to chemokine Stromal cell-Derived Factor-1 (SDF-1) expressed in the optic field (Jaurena, 2011). Additionally, in vitro and in vivo evidence indicated that a teratogenic level of ethanol exposure induces an aberrant ocular expression pattern of both SDF-1 and CXCR4, inhibiting the chemotactic response of NCCs to SDF-1 without affecting other morphometric or dynamic parameters (Jaurena, 2011).

The present report goes on to study factors involved in early colonization by cephalic NCCs invading the optic vesicle field to develop (among other derivatives) the ciliary ganglion. Neurotrophin-3 (NT-3), a member of the well-known neural growth factor family, is involved in multiple events of later neural development, including survival, proliferation and differentiation of neuronal precursors (Bernd, 2008). A new functional aspect of NT-3 was recently shown by our group, demonstrating a recovery of ethanol-induced abnormal NCC behavior by co-treatment with this neural growth factor (Jaurena et al., 2011). Some indirect evidence also suggested that NT-3 could be involved in the axonal guidance (Alto et al., 2009) and the migratory behavior of NCC derivative Schwann cells (Yamauchi et al., 2005) and enteric neurons (Chalazonitis, 2004). In vitro and in vivo approaches in the present work showed that cephalic NCCs migrate directionally up the NT-3 concentration gradient. The expression of NT-3 was shown in the ocular region and its canonical receptors on cephalic NCCs. Applying morpholino functional blocking technology to the whole-mount embryo it was shown an association between the altered expression of NT-3 in the optic vesicle, or the TrkC receptor blocking on the cephalic NCCs, and the perturbed distribution pattern of NCCs colonizing those target field.

Taken together with other complementary cell guidance factor(s), these results strongly suggest that the chemotactic mechanism is an essential element in the spatiotemporal orientation of NCCs toward specific regions of the embryo body. The data also amplify the functional scope of neurotrophic factors, involving them in new activities as molecular guides for the precise colonization of embryonic cells.

Materials and methods

Culture of cephalic neural crest cells

Primary cultures of NCCs were made as detailed elsewhere from chick embryos (*Gallus gallus*, Cobb line) incubated at 38 ± 1 °C in a humidified atmosphere up to stage HH 10 to 11 (Hamburger and Hamilton, 1951; Jaurena et al., 2011; Rovasio and Battiato, 2002; Rovasio et al., 2012). Briefly, after the cutting and opening of ectoderm, mesencephalic and rostral rhombencephalic NCCs were obtained by careful microdissection from the mass of cells bilateral to the neural tube, and transferred to a coverslip precoated with fibronectin (Rovasio et al., 1983). Cultures were incubated in Petri dishes (35 mm, Sigma Chem. Co., St. Louis, MO, USA) with 2 ml of N2 defined medium (Barnes and Sato, 1980) (N2 basal medium plus 5 μg/ml insulin, 100 μg/ml transferrin, 20 nM progesterone, 100 μM putrescine and 30 nM selenium in 100 ml of medium; Sigma Chem. Co.) supplemented with 10% fetal calf serum (FCS) (Sigma Chem. Co.) during 20 h at 37 ± 0.2 °C in 5% CO_2 in air. By applying the microdissection technique described, the degree of purity of NCC cultures was near 100%, without neural tube, ectoderm and/or mesoderm contaminants (see Fig. 5A, insets). If some culture contained tissue contaminants, they were detected by phase contrast microscopy and/or NCC immunolabeling (Rovasio and Battiato, 1995; Vincent et al., 1983) and consequently discarded. Some chemotactic assays were also performed with NCC cultures of 30 h or 40 h of incubation.

Chemotaxis assays

Agarose plug migration assay

This method was adapted from a previous description (Zhou et al., 2007). Briefly, prior to the experiment, a ring about 5 mm in length was cut from the broad end of a 200 μl plastic tip and silicone glued on the lateral wall of a 35 mm Petri dish, allowing a little angular cleft with the floor of the dish. Then, NCCs were obtained as explained, transferred to the Petri dish floor at about 500 μm from the glued tip and incubated with 1 ml N2 plus 10% FCS medium. After 20 h, 50 μl of 5% agarose (Sigma Chem. Co.) was placed into the tip segment, the culture medium of the dish was replaced with 1 ml of N2 defined medium, and 50 μl of 80 ng/ml Neurotrophin-3 (NT-3) in N2 medium was poured into the agar-containing tip. In other experiments, the NT-3 solution was replaced with heat-inactivated NT-3, or pre-incubated with 1–2 μg/ml of neutralizing antibody anti-NT-3 (Sigma Chem. Co.). This system allows the putative attractant to diffuse toward the culture medium, forming a two-dimensional concentration gradient, which is eventually detected by the cells (Zhou et al., 2007). After 3, 6 or 8 h of incubation, the cells were fixed and the proportion/distance of NCCs migrating in the fields toward and against the NT-3 gradient source was determined.

Video-microscopy assay

A real-time approach was applied using a computer-based video-microscopy system and software based on strictly proven objective directional criteria (Rovasio et al., 2012). Briefly, a coverslip carrying cultured NCCs was mounted upside down on a modified chemotaxis chamber and perfused with a concentration gradient of NT-3 (Sigma Chem. Co.) at the concentration of 20 ng/ml to 320 ng/ml in the source (or N2 medium = control). Other experiments were carried out with neurotrophic factor samples pre-incubated with 1–2 μg/ml of the corresponding neutralizing antibody anti-NT-3 (Sigma Chem. Co.), or with heat-inactivated molecules. Inhibition assays were also performed by pretreatment of cells with K252a, a potent inhibitor of Trk receptor phosphorylation (200 nM; Santa Cruz Biotech., Inc., CAL, USA) or REX antibody anti-p75 receptor (20 μg/ml; a generous gift of Dr. L. F. Reidchart, University of California, San Francisco, CA) for 40 min prior to chemotactic assay. To block Trk receptors, NCC cultures were incubated with specific antibodies (1/50; Santa Cruz Biotech.) for 10 min prior to chemotactic assay, which was carried out in the presence of the same concentration of antibodies in both wells of the chemotaxis chamber.

After mountings, the chamber was placed at 37 ± 0.1 °C in a video-microscopy system and real-time recorded for 6 h. Cell contours of each cell corresponding to the outgrowth NCCs were captured each 30 min and transferred to a computer using commercial software (SigmaScanPro, SPSS, Chicago, IL, USA) to analyze morphometric, dynamic and several chemotactic parameters, applying algorithms developed in our laboratory (Fabro et al., 2002; Rovasio and Battiato, 1995, 2002; Rovasio et al., 2012). Besides the proportion of migrating cells toward the putative attractants and the chemotactic index, other chemotactic parameters were tested under strict real-time directional criteria, such as the net distance traveled up the gradient, the turning angle of each cell trajectory and the angular bias of the whole cell trajectories (Fabro et al., 2002; Rovasio et al., 2012). Almost all results were coherent, without significant differences between the chemotactic parameters evaluated. Consequently, this report will show only the proportion of cells toward or against the NT-3 concentration gradients, and the chemotactic index expressing the efficient traveling of cells in relation to the attractant source. The chemotactic index was calculated as the quotient of the net distances parallel to the gradient (*X*-axis) of all the migrating cells, divided by the total distance traveled

(curvilinear distance) (Rovasio et al., 2012). For cells responding to a chemotactic gradient, the resulting value approaches a straight line (i.e. tends to 1), whereas for cells moving randomly the value tends to 0. For details of this method, see Rovasio et al. (2012). Chemotaxis assays were performed starting from NCC cultures of 20, 30 and 40 h. In addition, the NCC pathways were evaluated each hour of the total 6 h of the experiments. After videomicroscopy assay, as well as in some in-between sampling, NCC cultures were submitted to proliferation testing (see below). Moreover, as an operative routine, if a NCC divided during the cell-tracking evaluation, it was no longer recorded as a study sample.

Statistical analysis

After estimation of the minimal sample size, no fewer than 58 cells and a mean of 750 cell contours and centroids were studied in each experimental condition repeated in triplicate. Means comparisons were made with Student's *t*-test and nonparametric Mann–Whitney tests. Analysis of proportions was performed with the *z*-test with Yates correction, or previous transformation to the corresponding arc-sine values, and then one way ANOVA followed by Scheffé's method for comparing all contrasts, or the Tukey assay performed using the SigmaStat (SPSS, California, IL, USA) software. Statistical significance was set at $p < 0.05$.

Immunolabeling of NCC cultures

After washing with warm phosphate-buffered saline (PBS), the cells were fixed with 4% paraformaldehyde in PBS for 10 min at room temperature (RT). For NCC labeling, monoclonal anti-NC1 (Vincent et al., 1983) or HNK1 monoclonal antibody (Sigma Chem Co.) were used. For receptor labeling, cells were incubated for 2 h at RT with anti-TrkA (1/50), anti-TrkB (1/200) or anti-TrkC (1/50; Santa Cruz Biotech.) or overnight with anti-p75ntr REX (20 μg/ml) antibodies. For phosphorylated Trk receptors, NCCs were incubated under the same conditions as in chemotaxis assays, with 40 ng/ml NT-3 in the chamber source (or N2 medium = control). They were then fixed, as explained, with the addition of 0.25% Triton X-100 at zero time and after 6 h or 14 h of exposure to NT-3 gradient. After PBS washing, the same culture was incubated with phosphorylated Trk antibody (p-Trk, 1/100; Santa Cruz Biotech.) and with anti-actin antibody (H-196, 1/100; Santa Cruz Biotech.). Finally, cell cultures were incubated with a rhodamine or fluoresceine-isothiocyanate (FITC)-conjugated secondary antibody (1:100; Sigma Chem. Co.) for 1 h at 37 °C. Controls were performed by replacing primary or secondary antibodies with PBS or using heat-inactivated antibodies.

Cell viability assay

Cell survival was analyzed under different experimental conditions by the Live/Death Viability/Cytotoxicity Kit (Molecular Probes, Eugene, OR, USA). Briefly, NCC cultures were washed with PBS and incubated with 150 μl of 4 μM ethydium H-1 plus 2 μM calcein AM in PBS during 15 min at RT, then mounted with 10 μl of the same fresh work solution, and observed with a fluorescence filter for FITC. As a positive control, NCCs were pre-incubated with sodium azide. Cell images were obtained with an Olympus C7070 digital camera (Olympus Corp., Shinjuku-ku, Tokyo, Japan) and submitted to image analyses with the SigmaScanPro (SPSS, Chicago, IL, USA) software, according to previous descriptions (Jaurena et al., 2011; Rovasio et al., 2012). The viability index was calculated in a double blind manner as the proportion of live cells (calcein-positive cells = green) and dead cells (ethydium-positive cells = red) in the total number of cells, over all microscopic fields corresponding to the NCC halo of growing explants.

Proliferation assay

Cell proliferative capacity was assessed after incorporation of 5-bromo-2′-deoxyuridine (BrdU). Briefly, each culture was incubated with a final concentration of 10 μM BrdU for 3 h at 37 °C and 5% CO_2. After washing with PBS at room temperature, the cultures were fixed with 4% paraformaldehyde in PBS for 10 min, washed in PBS and permeabilized with 0.2% Tritón X-100 in PBS for 10 min. The cultures were rinsed in PBS and the DNA was denatured with 2 N HCl for 2 h at room temperature. After washing with 0.1 M borate buffer, pH 8.5, cultures were washed in blocking solution, then incubated with 1:100 dilution of anti-BrdU primary antibody (Santa Cruz, Biotech.) in a wet chamber for 20 h at room temperature, washed again with blocking solution and post-incubated with FITC-conjugate secondary antibody for 1 h at 37 °C. After washing with blocking solution, samples were mounted with anti-bleaching solution. As a negative control, the same procedure was performed omitting the primary antibody. Cell images were obtained as explained, and cell counts were made on an optical phase/FITC filter microscope. The proliferation index was calculated in a double blind manner as the proportion between the number of BrdU-positive cells and the total cell number in random fields comprising almost all the surface of NCC outgrowth.

Western blot

NCCs were obtained from 60 chick embryos as explained above, centrifuged at 10,000 xG, resuspended with 100 μl of RIPA buffer containing protease inhibitors, and homogenized in 200 μl of lysis buffer with syringe and 25G needle. After concentration by the chloroform/methanol method, the proteins were quantified (Bradford, 1976), resuspended with Laemmli buffer, and electrophoresed in 10% SDS/PAGE gels (Laemmli, 1970). Applying conventional technique, the separated proteins were transferred to nitrocellulose membranes (0.2 μm pore size; Bio-Rad Lab, Hercules, CAL, USA), blocked with 5% bovine serum albumin, immunolabeled, and the bound antibodies were detected by using chemiluminescence (Immun-Star C Kit; Bio-Rad Lab) on X-ray films (Medical X Ray Film, Agfa, Argentina).

Whole chick embryo

Obtaining and processing

The topographic distribution of bioactive molecules, markers and NCCs was assessed by whole-mount in situ hybridization and immunocytochemistry on chick embryos derived from fertile *Gallus gallus* Cobb-line chick eggs, incubated at 38 °C and 80% humidity for various periods of time, depending on the experimental schedule, to complete 40–45 h (stage HH 11) of embryo development (Hamburger and Hamilton, 1951).

In some experiments, a little window was cut in the shell and surrounding membranes to access the embryo, as described in current technical literature (Selleck, 1996), and then treated accordingly. In another lot of incubated eggs, the content of the whole egg was placed in a PBS containing bowl, the embryo and the surrounding membranes were excised 5 mm out of the vascular area, and washed in warm PBS, throwing away the vitelline membrane. Then the embryo was placed in a hemispherical dome, resembling the yolk curvature, of 4% agarose in N2 defined medium plus 10% FCS, and submitted to experimental handling and/or re-incubated in a wet chamber as described (Tolosa et al., 2012).

Fixation

After collecting and PBS-washing, the embryos were fixed with 4% paraformaldehyde in PBS for 4 h at 4 °C. For those embryos submitted to in situ hybridization, 0.1% diethylpyrocarbonate (DEPC)

(Sigma Chem. Co.) was added to all solutions. (DEPC was omitted in embryos used only for protein immunolabeling). Then, the embryos were washed in PBS (with/without DEPC) 3 × 10 min. The embryos running in the in situ hybridization method were dehydrated with an increasing methanol series (10 min in each: 50, 70, 2 × 95, 3 × 100%) and maintained in absolute methanol at −20 °C until use. Storing the embryos for 5 (or more) days improves the results, because the permeabilizing effect of methanol increases the penetration of reagents and probes. Those embryos submitted to immunolabeling were maintained in the post-fixation washing solution of PBS.

In situ hybridization

Whole mount in situ hybridization was performed as described (Tolosa et al., 2012). The production of digoxigenin-labeled antisense RNA probes was followed by their presentation to permeabilized chick embryos under suitable conditions for hybridization to occur. Probes were synthesized from a plasmid containing partial cDNA of chick NT-3 (kindly provided by Dr. F. Hallböök, Karolinska Institute, Stockholm, Sweden) (Hallbook et al., 1993) and from a plasmid containing the full-length cDNA of chick Slug (kindly provided by M. A. Nieto, Instituto Cajal, Madrid, Spain) (Del Barrio and Nieto, 2004). The subsequent development of the probe by means of a specific anti-digoxigenin antibody was followed by a color reaction, as a result of alkaline phosphatase activity using nitroblue tetrazolium/5-bromo-4-chloro-3-indolyl phosphate substrates (NBT/BCIP) (for reagents and technical details, see Sambrook et al., 1989; Tolosa et al., 2012).

Immunolabeling

The expression of specific mRNAs in the cell does not necessarily mean that the corresponding protein was synthesized and that it is functional. Therefore, in our experimental approaches, besides the detection of mRNA transcripts for NT-3 by in situ hybridization, it was also desirable to show the resulting protein expression by immunolabeling. This goal is not easy to reach, due to the very low concentration of the functional chemotactic proteins (Mortimer et al., 2008; Teves et al., 2006; Yu et al., 2009). In the present work, the primary antibodies used were: (1) Rabbit polyclonal anti-NT-3 (Sigma Chem. Co.) and (2) Mouse monoclonal anti-NC1 (Vincent et al., 1983) or HNK1 monoclonal antibody (Sigma Chem Co.) neural crest marker. Secondary antibodies were FITC-labeled goat anti-rabbit IgG, or rabbit anti-mouse IgGAM, or goat anti-mouse IgM (Sigma Chem Co.).

Briefly, after fixation and washing, the embryo was maintained in PBS solution and the ectoderm of the cephalic end was pierced with a tungsten microneedle to allow good antibody penetration. Alternatively, the whole-mount embryo was permeabilized with 1% Triton X-100 in PBS for 1–2 h, at RT, without evidence of significant differences with the piercing method. After the last PBS washing, the embryo was incubated in a wet chamber at RT with blocking solution (1% bovine serum albumin and 1.5% 0.2 M Glycine in PBS) 3 × 15 min, and then incubated with the corresponding primary antibody diluted in blocking solution at RT for 12 to 24 h, depending on the embryo age. After washing with blocking solution 3 × 30 min, the embryos were incubated with the FITC-conjugate secondary antibody for 8 to 16 h at RT depending on the embryo age. Then, they were washed 2 × 15 min with blocking solution and 3 × 15 min with PBS. All the previous technical steps were carried out in Petri dish series or, alternatively, the embryo was obtained and supported on a round filter paper which was mounted into a stainless steel holder device (Swinny filter holder 13 mm SS, Millipore, Billerica, MA, USA), and the top end of the filter unit was connected to a three-way stopcock to allow for changes of the environment containing fluids (for technical details, see Battiato et al., 1996).

Label determination

After in situ hybridization or immunolabeling, whole mount embryos were submitted to label analysis. Briefly, after the last PBS washing, the immunolabeled embryo was mounted on a glass slide using anti-bleaching medium (100 mg p-phenylenediamine, 90 ml glycerol and 10 ml PBS 4×) with a small square coverslip (5 mm × 5 mm) of Aclar® copolymer film (Electron Microscopy Sciences, Hatfield, PA, USA) to prevent the embryo being crushed, and observed with a fluorescence FITC filter (excitatory filter = 450–480 nm and barrier filter = 515 nm). The in situ hybridization embryo was similarly processed without the anti-bleaching treatment, and observed with a standard light microscopy optic. Whole mount embryo images were obtained with Olympus BX50 or confocal FV1000 microscopes, using an Olympus C7070 digital camera (Olympus Corp., Shinjuku-ku, Tokyo, Japan), or a Hamamatsu C2400 video-camera (Hamamatsu Photonics K.K., Tokyo, Japan). The distribution of NCCs on the whole mount embryo was calculated on the basis of Slug and HNK1 label density at prosencephalic/optic vesicle, mesencephalic and rhombencephalic levels. Fluorescent/densitometric labels were evaluated on images obtained with standard fluorescence and confocal microscopes (see below), using image analysis methods of public domain ImageJ (NIH, Bethesda, USA), and the SigmaScan-Pro software, and statistics according to SigmaStat (SPSS, Chicago, IL, USA), according to previous descriptions (Jaurena et al., 2011; Rovasio and Battiato, 2002; Rovasio et al., 2012). The same embryos were submitted to imaging with a conventional fluorescence system and with a confocal microscope. In the second case, images were recorded in 20 μm axial steps to perform a stack of 25 optical sections (Z-series). The fluorescent/densitometric data of stacked images were averaged and compared with the first group of conventional microscope images, and neither set of single and stacked images of the same embryo exhibited a significant label difference (data not shown).

Microinjection, electroporation and functional blocking

After the chick embryo was obtained (see above), it was submitted to the microinjection-electroporation protocols as described (Nakamura et al., 2004). Briefly, stages HH 8–10 embryos were utilized, prior to the start or in very early emigration of NCCs from the mesencephalic level. Treatments were made on both in ovo and ex ovo (agarose dome, see above) conditions, the results of which showed no significant differences. Using micromanipulators and under stereoscopic microscope, the microinjection of stages HH 9–10 embryos with 0.2–0.3 μl of 1 μM morpholino solution directed against Gallus gallus NT-3 mRNA (5′ to 3′ – GTAAGATCGTGGTAGGA GTAACCAT) (or morpholino control) (Gene Tools, LLC Philomath, USA), was localized unilaterally (dorsal up, right side) in the neural tube wall at the level of the future optic vesicle. The embryos, without posterior electroporation, were re-incubated for 10–15 h. In another group of stage HH 8–9 embryos, the microinjection of about 0.5 μl of 1 μM morpholino solution directed against Gallus gallus TrkC mRNA (5′ to 3′ –AGAGAGACATCCATCTCCGATTGCT) (or morpholino control) (Gene Tools, LLC, Philomath, USA) was localized in the lumen of the closing neural tube at the level of the future pro-mesencephalon. After administration, the micropipette was withdrawn and 0.5–1 ml of PBS was supplied to the embryo. Two platinum microelectrodes were slowly and carefully placed, resting 5 mm apart on each side of the pro-mesencephalic region of the embryo, and a squared wave of 18 V current was pulsed (50 ms On/50 ms Off) for 5 cycles, supplied from a ELP-5 electroporator (LIADE, FCEFN, Universidad Nacional de Córdoba, Argentina)

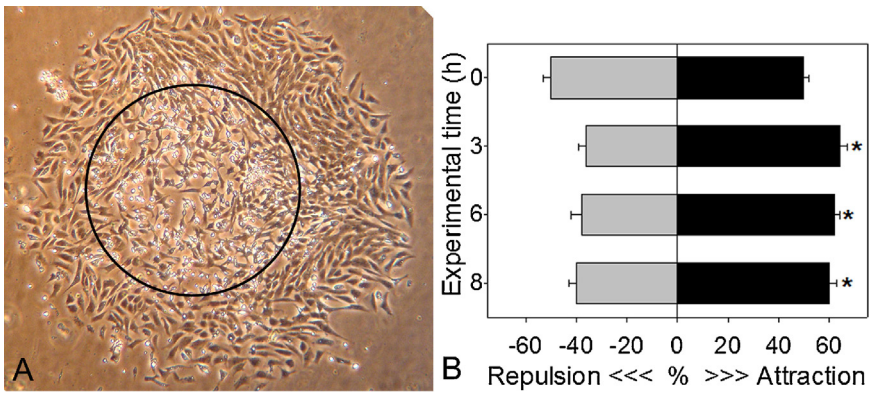

Fig. 1. Chemotaxis of NCCs with agarose plug method. (A) NCC initial culture (circle) and cell outgrowth after 8 h of incubation, showing the preferential migration toward the NT-3 source (right side). (B) Proportion of NCCs migrating toward (black bars) or against (gray bars) the NT-3 gradient after 3, 6 and 8 h incubation. *Significant difference vs. opposite side and vs. control ($p < 0.05$).

(Chesini et al., 2011). Following electroporation, the embryos were re-incubated in a wet environment for 10–15 h, then were collected and processed as explained to search for the morpholino localization and the distribution of NCCs by applying in situ hybridization and/or immunolabeling (see above).

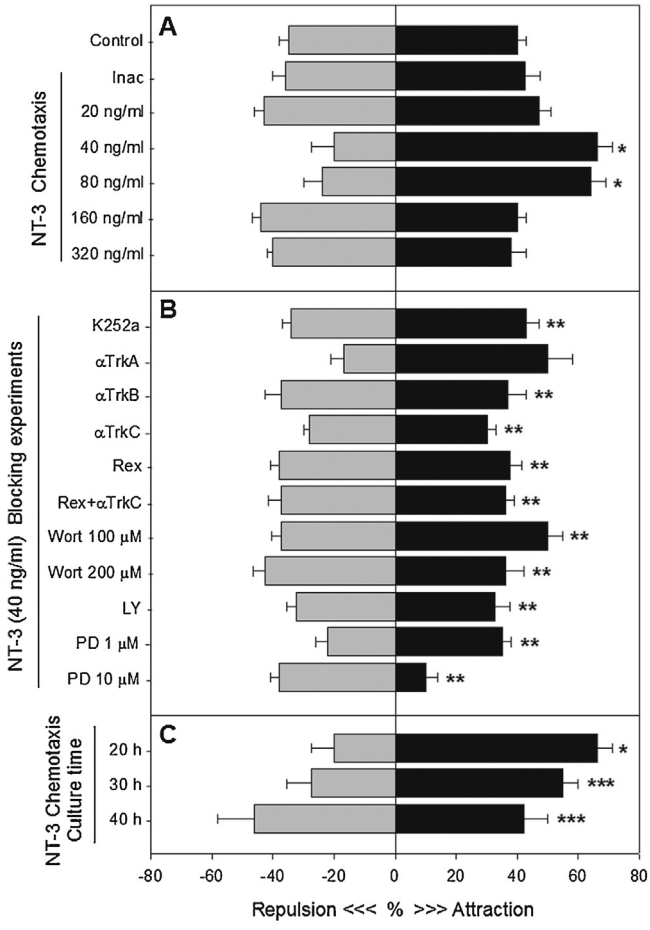

Fig. 2. Chemotaxis of NCCs in NT-3 gradients expressed as proportion of migrating cells. (A) Different initial concentrations of NT-3, control and inactivated (Inac) NT-3. Note the bell-shaped response, typical of chemotaxis (see details in 'Discussion' section). (B) Blocking experiments of Trks (K252a), TrkA (αTrkA), TrkB (αTrkB), TrkC (αTrkC), and p75 (Rex) receptors; inhibition of PI3K with Wortmanin (Wort) or LY29054 (LY), and inhibition of ERK signal with PD98059 (PD). (C) Proportion of migrating NCCs after different culture times. *Significant difference vs. Control. **Significant difference vs. NT-3 (40 ng/ml). ***Significant difference vs.NT-3 (40 ng/ml; 20 h culture time) ($p < 0.05$).

Another group of chick embryos was incubated until stage HH 9–10, then microbeads previously soaked with anti-TrkC receptor antibody (or N2 medium = control) were implanted in the pathway of mesencephalic NCCs. Microbeads (Affi-Gel Blue, Bio-Rad Lab., Hercules, CA, USA, or Heparin Sepharose CL-6B, GE Healthcare Bio-Sciences AB, Uppsala, Sweden) were washed with PBS and ethanol according to the manufacturers' instructions, centrifuged and soaked for 3–4 h at 4 °C with anti-TrkC antibody solution (2 µg/ml; Abcam Inc., Cambridge, MA, USA). After mounting the embryo on the agarose dome (see above) and using a tungsten microneedle, an incision of about 200 µm was made in the ectoderm layer at different levels (see Results) and parallel to the external edge of the mesencephalic neural tube. Microscopic controls were made before and after the re-incubation period to verify the microbeads' position.

Results

NT-3 elicits chemotactic behavior of in vitro NCCs

In a group of in vitro experiments, cephalic NCCs were submitted to an exogenous gradient of NT-3 diffusing from an agarose plug. Migrating cells toward the NT-3 source were compared with a control condition in which the neurotrophic factor was replaced with N2 defined medium. The proportion of NCCs migrating toward and against the NT-3 source was also assessed in the same culture system. After incubation for 3, 6 or 8 h, 60% of cells climbed the NT-3 gradient, compared to about 40% of NCCs migrating against the NT-3 source, or to 50% of the control condition. In both cases the differences were statistically significant, thus suggesting a vector-oriented cell migration (Fig. 1).

This encouraged us to apply a more efficient method to investigate oriented cell migration, based on a real-time video-microscopy platform and strict directional criteria (Rovasio et al., 2012). After NCC cultures were mounted in the chemotaxis chamber, initial concentrations of 20 to 320 ng/ml of NT-3 were loaded in different experiments, and recorded during 6 h. Cell trajectories were tracked and various chemotactic parameters were calculated. Since the values of Proportion of migrating cells, Chemotactic index, Net distance traveled up the gradient, Turning angle of each cell trajectory and Angular bias of the whole cell trajectories (Rovasio et al., 2012), converged toward equivalent results, only Proportion of migrating cells and Chemotactic index, expressing the efficient distance traveled by a cell in relation to the attractant source, will be used throughout this article.

NCCs exhibited a strong chemotactic response at initial concentrations of 40 and 80 ng/ml of NT-3 in the source of the gradient, expressed as both the proportion of migrating cells (Fig. 2A) and

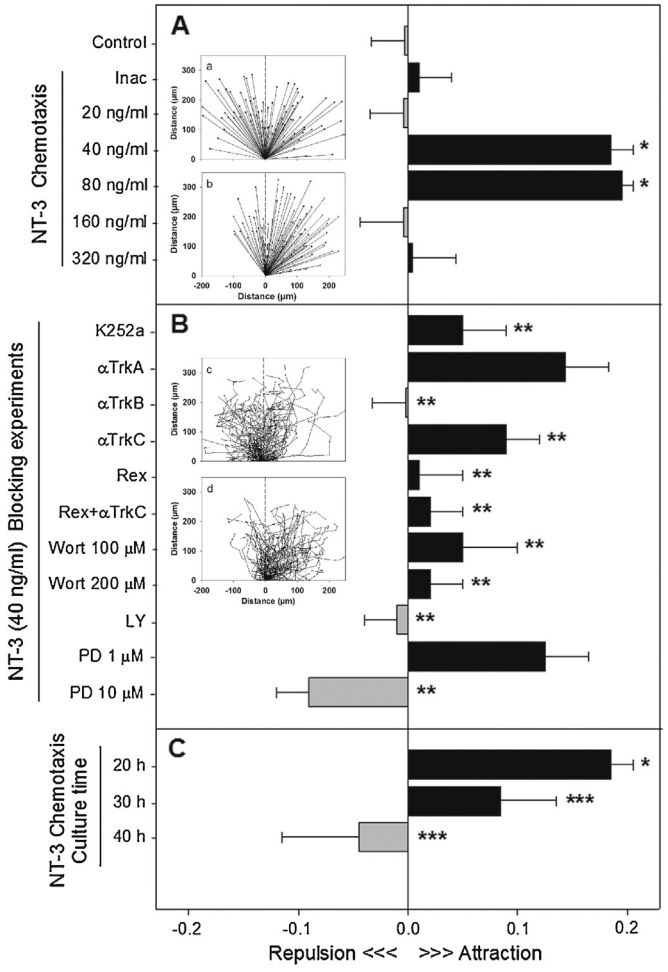

Fig. 3. Chemotaxis of NCCs in NT-3 gradients expressed as chemotactic index. (A) Different initial concentrations of NT-3, control and inactivated (Inac) NT-3. Note the bell-shaped response, typical of chemotaxis (see details on Discussion section). Insets show linear distance/turning angle on control condition (a) and NCC cultures exposed to gradient of NT-3 (80 ng/ml) (b). (B) Blocking experiments of Trks (K252a), TrkA (αTrkA), TrkB (αTrkB), TrkC (αTrkC), and p75 (Rex) receptors; inhibition of PI3K with Wortmanin (Wort) or LY29054 (LY), and inhibition of ERK signal with PD98059 (PD). Insets show cell tracks of individual cells of typical experiments on control condition (c) and NCC cultures exposed to gradient of NT-3 (80 ng/ml) (d). (C) Chemotactic index of migrating NCCs after different culture times. *Significant difference vs. Control. **Significant difference vs. NT-3 (40 ng/ml). ***Significant difference vs. NT-3 (40 ng/ml; 20 h culture time) ($p < 0.05$).

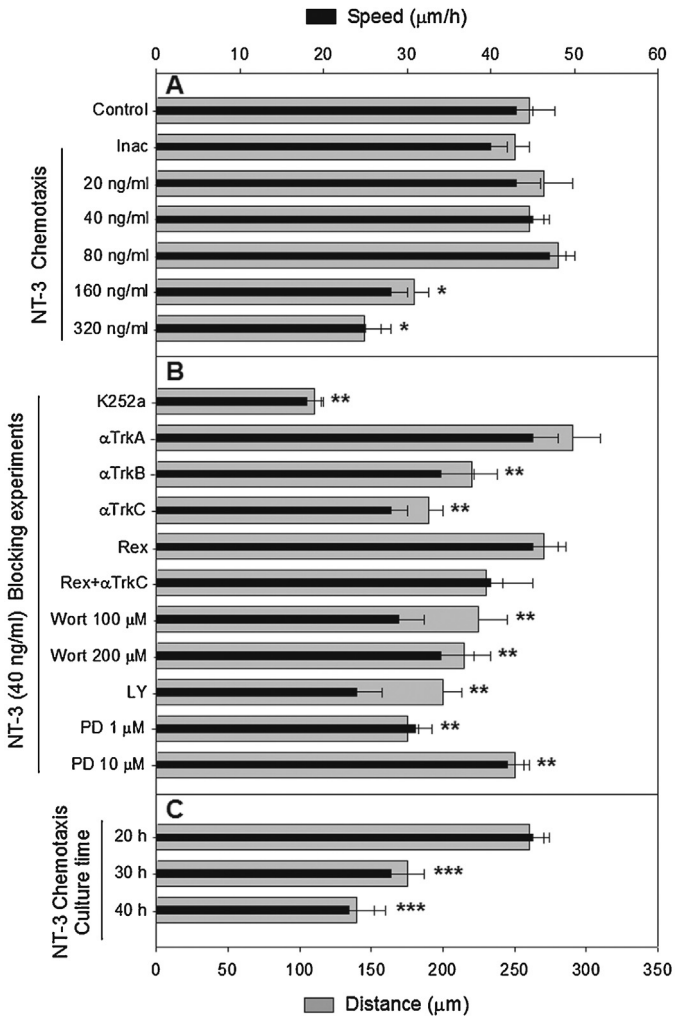

Fig. 4. Absolute dynamic parameters of NCCs in NT-3 gradients expressed as distance traveled (gray bars) and cell speed (black bars). (A) Different initial concentrations of NT-3, control and inactivated (Inac) NT-3. (B) Blocking experiments of Trks (K252a), TrkA (αTrkA), TrkB (αTrkB), TrkC (αTrkC), and p75 (Rex) receptors; inhibition of PI3K with Wortmanin (Wort) or LY29054 (LY), and inhibition of ERK signal with PD98059 (PD). (C) Distance traveled and cell speed of migrating NCCs after different culture times. *Significant difference vs. Control. **Significant difference vs. NT-3 (40 ng/ml). ***Significant difference vs. NT-3 (40 ng/ml; 20 h culture time) ($p < 0.05$).

the chemotactic index (Fig. 3A, see also Bc,d). The proportion of chemotactic cells (64–66 ± 5%) supports the results obtained with the agar plug method. At higher or lower concentrations of NT-3, as well as in the control conditions, the proportion of oriented cells fell to about 40–45%, with the percentage of cells almost equivalent toward both sides of the chemotaxis chamber. Since there were no significant differences between treatments with NT-3 pre-incubated with anti-NT-3 antibody or heat-inactivated NT-3, the values of these conditions were shown as inactivated NT-3 (Figs. 2A and 3A, Inac). It should be noted that the sum of the proportion of cells migrating toward and against the gradient is not 100%. That is due to the criteria established in our system to determine and quantify chemotactic parameters, under which the complementary value to reach 100% corresponds to that of non-oriented cells (see Rovasio et al., 2012). Also, the directional-based chemotactic index clearly showed the highly oriented migratory behavior of NCCs submitted to gradients of 40 and 80 ng/ml NT-3 in the source, as well as values close to zero at lower or higher concentrations and in the control conditions (Fig. 3A, see also Bc,d).

While the chemotactically oriented NCCs up to NT-3 were expressed at 40 and 80 ng/ml of neurotrophic factor, the distance traveled and cell speed under these experimental conditions maintained values similar to the control conditions and at the lower NT-3 concentration, even if there was a reduction of these absolute dynamic parameters at higher concentrations of NT-3 (Fig. 4A). Possible associations between low chemotactic behavior and cell death were discarded, as the viability assay showed no significant differences in cell survival between the different experimental conditions, this being equal to or higher than 90% in all the experiments. Moreover, it is obvious that in the dynamic parameter assays only moving (thus, live) cells were computed. On the other hand, the proliferation test performed in all experimental conditions revealed no significant differences, indicating that the number of NCCs does not affect the results obtained.

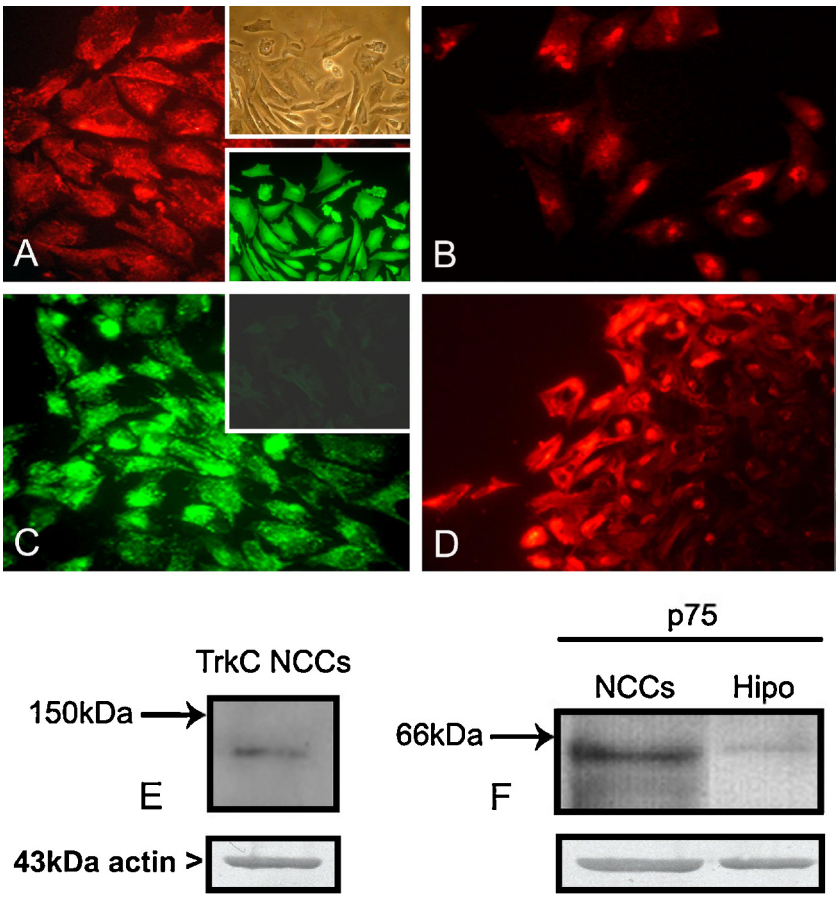

Fig. 5. Expression of TrkA (A), TrkB (B), TrkC (C) and p75 (D) receptors on in vitro cephalic NCCs. Insets on A show phase contrast (top) and HNK-1 immunolabelling (bottom) of the same field, as NCC purity control. Inset in (C), shows a NCC culture exposed to inactivated anti-TrkC antibody. All NCC cultures treated with inactivated primary antibodies have the same aspect. Western blot expression of TrkC (E) and p75 (F) receptors of NCCs. Hippocampus (Hipo): positive control for p75 receptor. Actin: loading control.

Trks and p75 receptors are involved in chemotaxis of NCCs up to NT-3

It is known that TrkC and p75 are canonical receptors for NT-3, which can also bind to TrkA and TrkB if this neurotrophic factor is offered at high concentrations (Mischel et al., 2001). Specific immunolabeling enabled us to observe that cephalic NCCs express different levels of TrkA, TrkB, TrkC and p75 receptors, with TrkC and p75 receptors being more constantly and homogeneously expressed (Fig. 5A–D), while this was not seen in the controls (Fig. 5C, inset). The expression of the latter receptors by NCCs, at the stage of development studied here, was also confirmed by western blot analysis (Fig. 5E and F).

Knowing that NCC chemotaxis is elicited by concentration gradients of NT-3, and that neurotrophic receptors express on NCCs, we conducted assays with the aim of blocking those functional behaviors. When the inhibitor K252a prevented the phosphorylation of Trk receptors, the NCCs no longer responded chemotactically to NT-3 (Figs. 2B and 3B). Moreover, after immunoblocking of TrkB and TrkC receptors, NCCs failed to exhibit chemotactic migration up to NT-3, while inhibition of TrkA receptor did not seem to significantly affect the oriented cell migration (Figs. 2B and 3B). These changes were observed equally when oriented migration was expressed as the proportion of cells (Fig. 2B) and as the chemotactic index (Fig. 3B). On the other hand, the absolute dynamic parameters, distance traveled and cell speed, were also significantly diminished when TrkB and TrkC receptors on NCCs were blocked (Fig. 4B).

In the NT-3 chemotaxis experiments of NCCs incubated with the anti-p75 function blocking Rex antibody, oriented cell migration was significantly reduced as compared to control conditions (Figs. 2B and 3B). Moreover, when NCCs were treated with both anti-TrkC and anti-p75 antibodies, the result was also a significant reduction of chemotactic behavior (Figs. 2 and 3B). Curiously, after blocking the p75 receptor, the NCCs not responding chemotactically to NT-3 remained as a random migration population, traveling the same distance and cell velocity as the control or NT-3 chemotactically guided cells (Fig. 4B).

NT-3 ligands activate signal chain related to NCC chemotactic migration

NCC cultures exposed to an NT-3 (40 ng/ml) gradient showed phosphorylated Trk receptors at the cell periphery during the chemotaxis assay, while after a longer time the immunolabel was seen to be internalized into the cytoplasmic milieu (Fig. 6).

After the evidence of NT-3-dependent phosphorylated Trk receptors during the chemotactic response of NCCs, incubation with Wortmanin or LY29054, inhibitors of phosphatidylinositol 3′-kinase (PI3K), was shown to induce a significant concentration-dependent diminution of NCC chemotactic migration compared to controls, both in the proportion of migrating cells (Fig. 2B) and in chemotactic directional travel (Fig. 3B). Moreover, after PI3K blocking, the absolute parameters of distance traveled and cell speed showed a significant reduction (Fig. 4B).

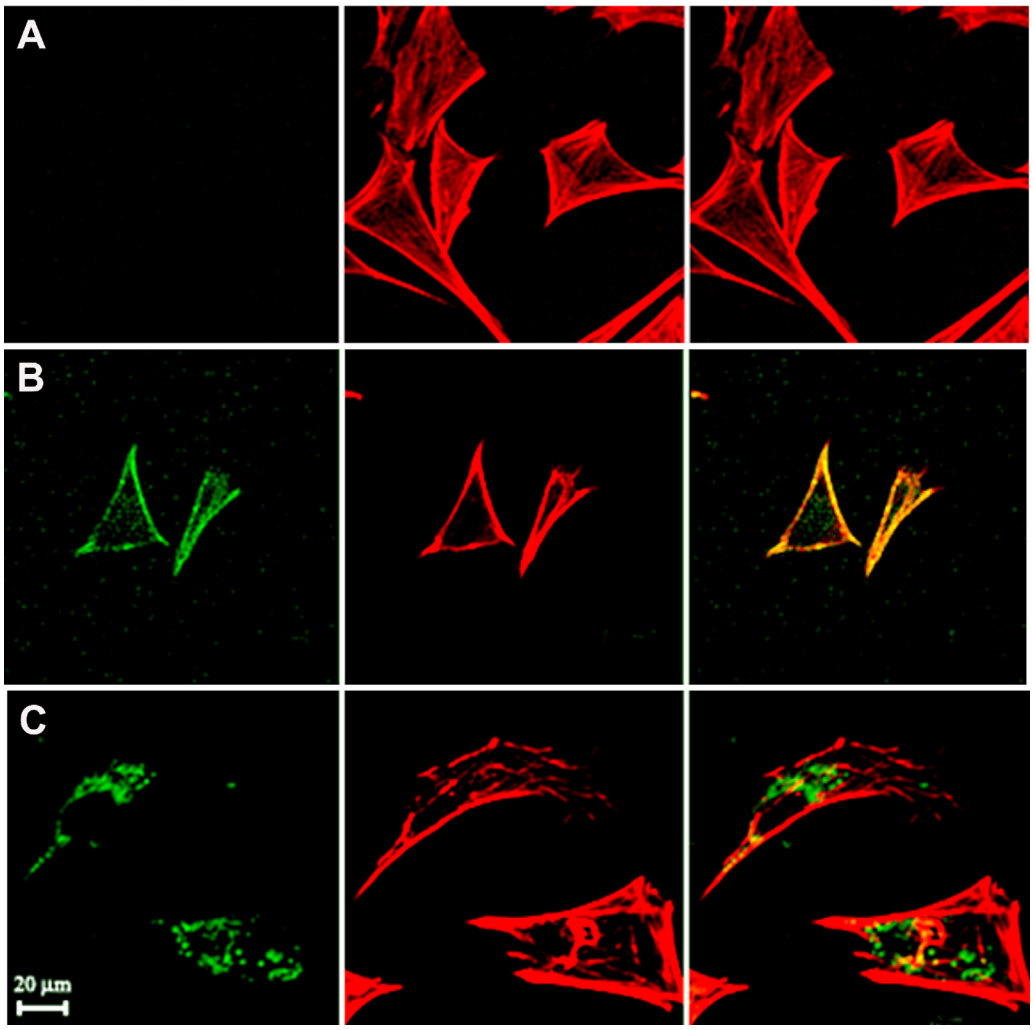

Fig. 6. Activated Trk-receptors during the chemotaxis assay. Immunolabeling of phosphorylated Trk receptors (green) and actin molecule (red) at zero time (A) and after 6 h (B) or 14 h (C) of exposure to NT-3 gradient. Phosphorylated Trk receptors delineate the cell periphery during chemotactic response, then apparently were internalized.

On the other hand, when the NT-3/NCCs system was tested in the presence of PD98059, inhibitor of the ERK signal chain, a concentration-dependent effect was seen on the chemotactic behavior of NCCs. A light but significant NCC chemotaxis up to NT-3 was evident with 1 μM concentration of the inhibitor, clearly evidenced in the chemotactic index (Fig. 3B). Moreover, chemo-repulsive cell migration was seen after incubation with 10 μM PD18059, both in the proportion of migrating NCCs (Fig. 2B) and in the directional parameter (Fig. 3B). Meanwhile, there was a reduction in absolute dynamic parameters, distance traveled and cell velocity, and these were even lower in the experiments using the lower concentration of the ERK-inhibitor (Fig. 4B). It is worth noting that, in all signal chain blocking experiments, the viability assay showed no significant differences of cell survival between controls and experimental conditions.

Chemotactic behavior up to NT-3 depends on NCC culture time, resembling the timing of the in vivo condition

In experiments using NCCs from progressively longer periods of initial culture times (>20 h), we observed a diminution of chemotactic response to NT-3 in cultures of 30 h, and a fall to control values in 40 h NCC cultures. This significant lowering of chemotactic responses of "older" cells was observed in both the proportion of responder cells and the directional chemotactic index (Figs. 2C and 3C). In addition, NCCs from 40 h of culture time showed clear chemo-repulsion against the NT-3 gradient (Fig. 3C). The distance traveled and the cell speed of NCCs in the NT-3 gradient also showed a significant culture time-dependent reduction (Fig. 4C). The viability assay showed no significant differences of cell survival between these different NCC culture times.

When NCC cultures with 20 h of initial incubation were exposed to NT-3 gradient and evaluated each hour during the usual experimental time of 6 h, we observed that the chemotactic behavior of NCCs for the first 60 min was constantly maintained without significant changes until the end of the 6 h recording (Fig. 7A). Moreover, the absolute dynamic parameters distance traveled and cell velocity showed no significant differences throughout these experiments (Fig. 7B).

In vivo expression of NT-3 in target field and TrkC/p75 receptors in NCC region

By applying in situ hybridization in whole-mounted chick embryos, we found a constant expression of mRNA for NT-3 at the pro-mesencephalic boundary, as well as in the caudal wall and stalk of the optic vesicle in stages HH 10–12 (Fig. 8A). Moreover, whole-mount embryo immunolabeling showed a constant expression of TrkC and p75 receptors (Fig. 8C–E) in the cephalic field of NCCs (Fig. 8B). Applying immunolabeling after a long exposure with

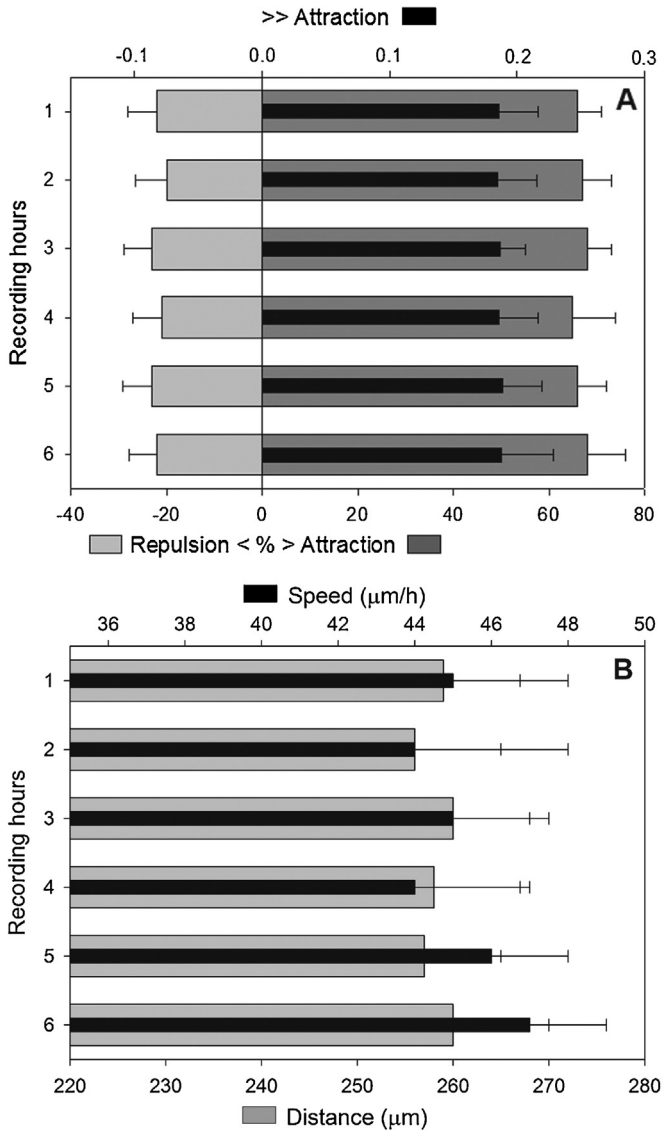

Fig. 7. (A) Chemotactic parameters of NCCs in NT-3 gradient (40 ng/ml) expressed as proportion of migrating cells (gray bars) and chemotactic index (black bars) evaluated each hour during 6 h. (B) Absolute dynamic parameters of NCCs in NT-3 gradient (40 ng/ml) expressed as distance traveled (μm; gray bars) and cell velocity (μm/h; black bars) evaluated each hour during 6 h. The values among hours of tracking are not significantly different.

the specific antibody as well as a prolonged recording time, NT-3 protein was also observed diffusing from the optic vesicle field (Fig. 9).

Blocking cephalic expression of NT-3 or NT-3 receptors in the whole-mount embryo perturbs NCC distribution

Following the above results indicating that NT-3 gradients stimulate chemotactic migration of cephalic NCCs, and that cell directionality response clearly associates with the expression of NT-3 at the target site of cephalic NCCs and the corresponding receptors on NCCs, the next experimental stage was to perform a functional blocking of this system. After the morpholino against NT-3 was unilaterally microinjected into the neural tube wall at the level of the future optic vesicle of whole-mount chick embryos, a perturbed distribution of cephalic NCCs was observed (Fig. 10).

After about 10 h of morpholino supply, the embryos were harvested and submitted to in situ hybridization for NCC Slug marker or HNK-1 immunolabeling, in order to evaluate the distribution of this cell population, having the contralateral side as internal control. Comparing the electroporated right side (Fig. 10A and B) with the left side of the same embryo or with control embryos, a clear and significant lower number of NCCs were found colonizing the optic vesicle region when the NT-3 blockade was induced by the specific morpholino (Fig. 10D, graphs), compared with the opposite side or with the morpholino control embryo (Fig. 10C, graphs). Moreover, in the mesencephalic segment of NT-3-morpholino-supplied embryo, significantly higher NCC labeling was observed on the right side, corresponding to the NT-3 blocking side (Fig. 10D, graphs). This bilateral difference was not observed in control embryos, in which the NCC population was equivalently distributed on both sides of the cephalic region (Fig. 10C, graphs). At rhombencephalic level, NCCs were equally distributed on both sides of the morpholino or control embryos (Fig. 10C, D, graphs). It should be noted that the same results were obtained when using the Slug in situ hybridization marker (Fig. 10) or the HNK1 antibody to label the NCCs.

On the other hand, when equivalent studies were made on whole-mount embryos treated with morpholines against TrkC receptors, results similar to the above were obtained (Fig. 11). It is well known that the neural tube intraluminal microinjection meets in direct contact the delivered molecules with the presumptive pre-migratory NCCs (Del Barrio and Nieto, 2002; Hammerle and Tejedor, 2007). When these embryos were evaluated after unilateral electrotransfection with morpholino against mRNA of TrkC (Fig. 11) or p-75 (not shown), the mesencephalic NCCs showed an early abnormal distribution (Fig. 11B). The NT-3 receptor blockade was followed after several hours post-incubation by perturbed migration to the optic vesicle region, compared with the contralateral control side (Fig. 11A).

Moreover, chick embryos implanted with a source of blocking NT-3-receptor TrkC in the migratory pathway of mesencephalic NCCs, clearly showed a perturbation of the normally oriented migration of a population of NCCs toward the optic vesicle (Fig. 12). At the caudal levels of the mesencephalic region, an ectopic source of N2 medium (control) as well as the TrkC antibody-embedded beads did not show significant perturbation of the normal distribution of NCCs (Fig. 12A and B). On the other hand, when the anti-TrkC antibody-soaked beads were implanted at a mesencephalic level near the "influence zone" of the optic field, the corresponding NCCs exhibited a clear diminution of migratory orientation toward the optic vesicle, compared with the contralateral non-treated side of the same embryo (Fig. 12C and D) and with a contralateral side implanted with beads carrying the N2 control (not shown), which exhibited a topography equivalent to that of the control embryos (Fig. 12A and B). Also, the sub-population of mesencephalic NCCs, not allowed to go toward the optic vesicle, seemed to accumulate at the right side lateral mesencephalon (compare with Fig. 10D). The perturbed normal distribution of NCCs in the vicinity of the anti-TrkC antibody source as well as the diminished migration toward the optic vesicle region (Fig. 12D, OV, right arrow), support the view that they lose precision on their way toward the ocular target field.

Discussion

Embryonic cell orientates to defined regions

The ability of the embryonic cell to distribute into particular regions of the body is a principal, fascinating and intricate problem of dynamic developmental biology. Although many reports have revealed where and by what ways embryonic cells distribute, the research is as yet scarce about how and why they orientate with

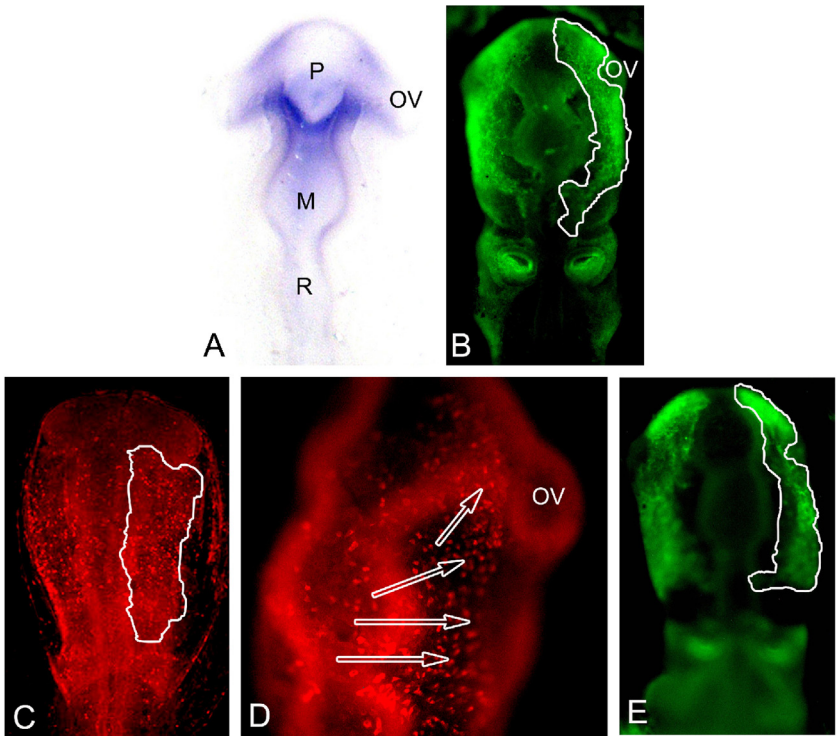

Fig. 8. Whole mount embryo expression of the NT-3/NCCs chemotaxis system. (A) In situ hybridization for NT-3 in the optic vesicle field. (B) Immunolabeling of NCCs. (C and D) Immunolabeling of TrkC receptor. (E) Immunolabeling of p75 receptor. White outlined: NCC area (right side). Arrows: general pathways of cephalic NCC migration (see also Le Douarin and Kalcheim, 1999; Lee et al., 2003). (A–C and E) Dorsal view. D: oblique dorsal-right view. OV: optic vesicle. P: Prosencephalon. M: Mesencephalon. R: Rhombencephalon.

high precision toward defined sites, sorting among innumerable signal molecules of their micro-environment.

The old concept of chemotaxis, proposed by Santiago Ramón y Cajal at the end of the 19th century for directional axon growth cones (Ramón and Cajal, 1892), is a plausible process that may help to answer queries about the directional communication of the embryonic cell (Rovasio et al., 2012). This mechanism is centered on cell capacity to recognize guide signals arising from a spatiotemporal concentration gradient, and responding consequently with oriented locomotion toward specific soluble

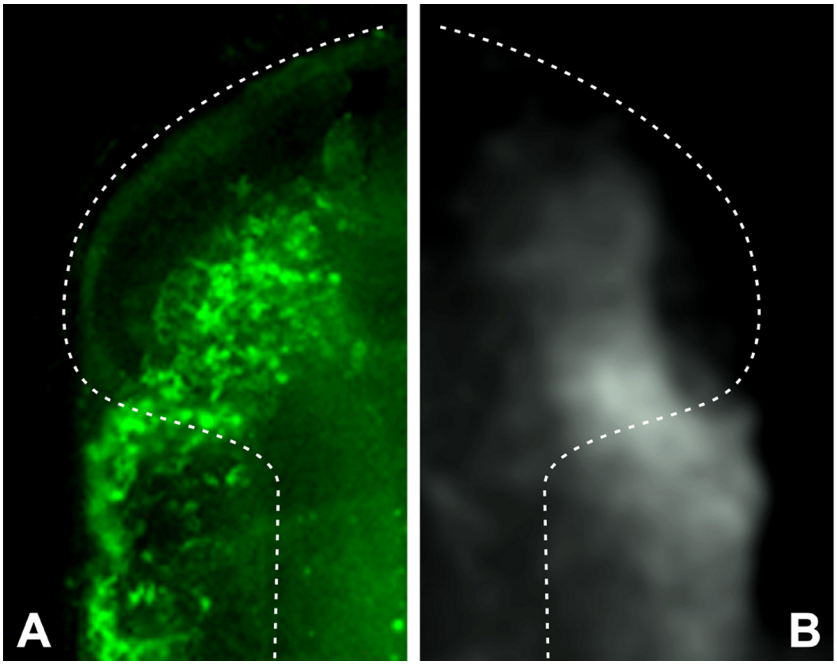

Fig. 9. Whole mount embryo expression of the NT-3/NCCs chemotaxis system. (A) Pro-mesencephalic region of chick embryos at stage 10–11 HH. Immunolabeling of NCCs arriving in the ocular region (HNK1 monoclonal antibody). (B) Same level at the equivalent embryo stage. Immunolabeling of NT-3 protein expression diffusing from the optic vesicle stalk area, after a long exposure with anti-NT-3 antibody and prolonged recording time. White broken line: outline of the neural tube at cephalic end.

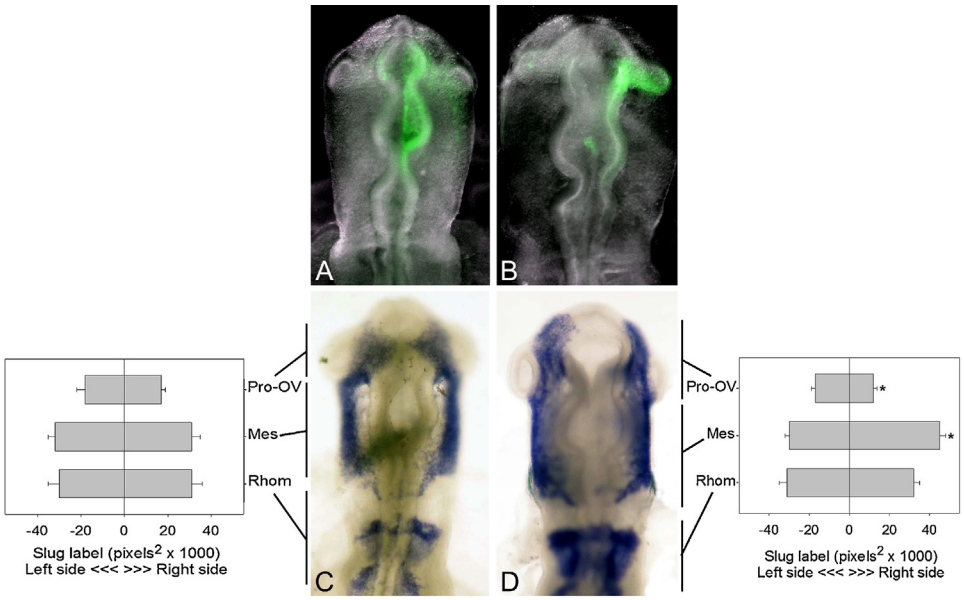

Fig. 10. NT-3 blocking on whole-mount chick embryos supplied with morpholino at stage HH 9–10 and studied at stage HH 11–12. (A) Embryo treated with control morpholino. (B) Embryo treated with morpholino to NT-3. Note that, after unilateral microinjection, morpholino localizes at the right side of the embryo (green). (C) Control morpholino. (D) NT-3 morpholino. In situ hybridization to Slug marker to show NCC populations at the prosencephalic/optic vesicle (Pro-OV), mesencephalic (Mes) and rhombencephalic (Rhom) levels. Graphs show quantitative data of densitometric Slug-labeled NCCs colonizing each of the indicated segmental levels. Results from immunolabeling with HNK1 antibody show an equivalent NCC distribution as described. *Significant difference vs. Control and vs. the opposite side ($p < 0.05$).

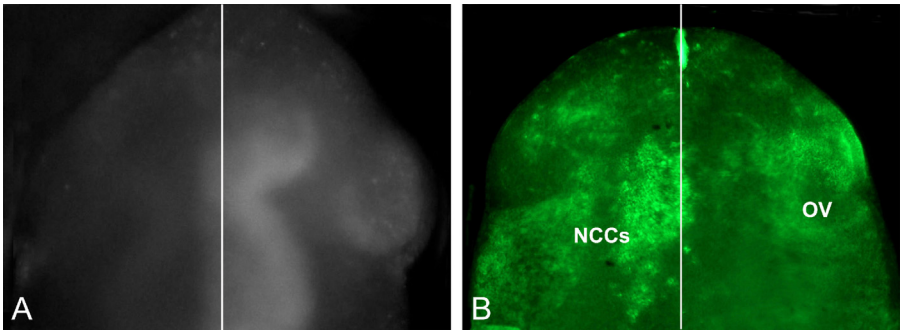

Fig. 11. TrkC receptor blocking on whole-mount chick embryos supplied with morpholino at stage HH 9 and studied at stage HH 11. (A) Embryo delivered with morpholino to mRNA TrkC. After electroporation, morpholino localizes at the right side of the embryo. (B) After re-incubation period, embryos treated with TrkC-morpholino showed arrested migration of NCCs toward the right side optic vesicle (OV) region, while these distribute normally on the control left side. Immunolabeling with HNK1 antibody. Vertical line indicates the sagittal axis. On embryos injected with control morpholino, NCCs distribute equally on both sides (not shown).

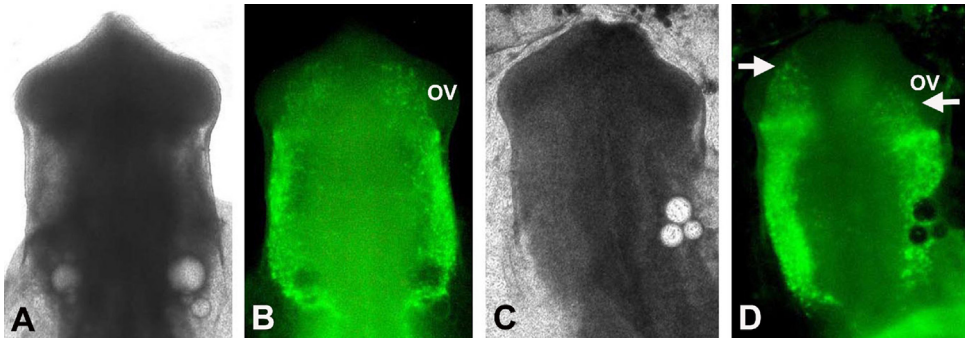

Fig. 12. Mesencephalic NCCs distribution after NT-3 signal perturbation. (A and B) Phase contrast (A) and HNK1 immunolabeling for NCCs (B) of a chick embryo inserted at the caudal end of mesencephalic region with microbeads soaked with N2 medium (control, left side) and with antibody anti-TrkC receptor (right side). There was no perturbation of the normal distribution of cephalic NCCs. (C and D) Phase contrast (C) and HNK1 immunolabeling (D) of a chick embryo inserted at the right side of the mesencephalic region with microbeads soaked with an antibody anti-TrkC receptor. The distribution of NCCs was severely perturbed, showing arrested migration in the vicinity of the beads as well as diminished distribution toward the optic vesicle region (OV, right arrow), compared with the control left side, in which distribution of NCCs was normal (left arrow).

factor(s) segregated by "target" fields. Chemotaxis was recently re-discovered by researchers and spectacular contributions have been made concerning the pathfinding behavior of the axon growth cone (Alto et al., 2009; Charron and Tessier-Lavigne, 2005; Gore et al., 2008; Mortimer et al., 2008), primordial germ cells (Molyneaux and Wylie, 2004; Ricardo and Lehmann, 2009), lateral line primordium (Breau et al., 2012; Streichan et al., 2011), sperm cells (Guidobaldi et al., 2012; Teves et al., 2006; Wolfner, 2011) and other cell populations (von Philipsborn and Bastmeyer, 2007), including neural crest cells (NCCs) and their derivatives (Jaurena, 2011; Kasemeier-Kulesa et al., 2010; Kulesa et al., 2010; Mayor and Theveneau, 2013; McLennan et al., 2012; Natarajan et al., 2002; Rezzoug et al., 2011; Rovasio et al., 2012; Tolosa, 2013; Tolosa et al., 2012; Tosney, 2004; Zanin, 2011).

NCCs are a well-known example of an accurately moving paradigm, since this embryonic multipotent cell population of vertebrate embryos undergoes wide dispersion along multiple pathways, invading and colonizing defined sites of the body with high precision, to differentiate into many derivatives (Le Douarin and Kalcheim, 1999). Experimental evidence supports the chemotactic response of NCCs to the trophic factors Glial-derived neurotrophic factor (Natarajan et al., 2002) and Stem cell factor (SCF) (Rovasio et al., 2012), to the chemokine Stromal cell-derived Factor-1 (SDF-1) (Jaurena, 2011; Rezzoug et al., 2011), and to the morphogen Sonic hedgehog (Shh) (Tolosa, 2013). Now we hope to provide valuable data on NCC directional cell behavior induced by Neurotrophin-3 (NT-3) (Zanin, 2011). This member of the neurotrophic factor family participates in several functional activities at early stages of embryo development as well as in mature organisms (Gilbert, 2003), also playing a chemotactic role in the axonal growth cone (Alto et al., 2009; Paves and Saarma, 1997) and NCC-derived cells (Chalazonitis, 2004; Yamauchi et al., 2005).

In vitro data support the directional moving of NCCs

The present work shows the chemotactic response of cephalic NCCs confronted in vitro with gradients of NT-3 as determined by a real-time strict directional-based technology (Rovasio et al., 2012). This oriented cell behavior was clearly shown in a subpopulation of NCCs, with parameters involving different expressions of directional cell migration, such as the proportion of oriented cells, the distance traveled toward the attractants, the angular bias of the cell trajectories and the chemotaxis index. All these parameters form a bell-shaped curve (see Figs. 2A and 3A), which is typical of concentration-dependent chemotactic behavior (Erlandsson et al., 2004; Gore et al., 2008; Guidobaldi et al., 2008; Teves et al., 2006; Rovasio et al., 2012). This response to a concentration gradient does not produce a saturation curve of chemotaxis because, when the attractant concentration increases above saturation, specific membrane receptors remain totally occupied, are thus incapable of detecting differential changes coming from the extracellular gradient and, consequently, the chemotactic response falls. The bell-shaped curve was constantly found in the proportion of responding NCCs, in the distance traveled and the bias of the cell-tracking angle toward the source of the NT-3. This characteristic may also enable us to speculate that it is involved in the arrest of migratory behavior at the final ("target") site, or to partially explain the as yet little understood mechanism of chemo-repulsion (see below).

Several molecules and mechanisms were proposed as working for the efficient locomotion of NCCs, from extracellular matrix molecules (Lock et al., 2008; Rovasio et al., 1983), to cell-to-cell contacts (Teddy and Kulesa, 2004), planar cell polarity (Matthews et al., 2008) and the mechanism of contact inhibition of locomotion (Carmona-Fontaine et al., 2008). These and other studies, using recent technologies on in vivo embryos, provide valuable data for understanding the migration of NCCs (Kulesa et al., 2010; McLennan et al., 2012). However, although they are important constituents of migratory behavior, they may be factors that are not responsible but rather cooperative for oriented cell motility. Our in vitro results, obtained with a system that enables the study of NCC subpopulations confronted with concentration gradients of attractants, and excluding other migratory factor(s), clearly showed that chemotaxis, studied under strict real-time directional criteria, may be an essential contribution to spatiotemporal orientation of NCCs toward specific fields of the embryo (Rovasio et al., 2012). In addition, in this sensitive process of NCC guidance, it is also reasonable to consider the confluent (also redundant) mechanisms governed by other growth factors (Rovasio et al., 2012), chemokines (Jaurena, 2011) and/or morphogens (Tolosa, 2013), providing for any failures in the directional behavior of embryonic cells.

As a part of this rationale, it is also important to note that, in this work (as in almost all "chemotactic papers"), we could not find 100% of the neural crest population responding to NT-3. This is coherent with the idea that early NCCs are a heterogeneous cell population that may respond to several guiding cues (Jaurena, 2011; McLennan et al., 2012; Rezzoug et al., 2011; Rovasio et al., 2012; Tolosa, 2013). It is thus quite feasible that diffusible factors arising from regions of the anatomofunctional final destination of mesencephalic NCCs (putative sites for ciliary ganglion, cartilage, bone and elements of peripheral nervous system of the craniofacial field; Le Douarin and Kalcheim, 1999), could be an important aid to NCCs finding their correct pathway(s).

Forward or backward, that's the question...

Besides the evidence supporting the chemotaxis of NCCs toward a concentration of 40 and 80 ng/ml of NT-3 at the source of the gradient, the cells exposed to lower (20 ng/ml) or higher (160–320 ng/ml) concentrations showed arrested migration in relation to the gradient (the abovementioned bell-shaped chemotactic curve). On the other hand, a chemorepulsion effect (or fugetaxis) was evident in certain experimental conditions, such as a heavy blockade of the ERK signals or the use of "old NCCs" of 40 h culture time (see below and Figs. 2 and 3B and C). The chemorepulsive phenomenon has been studied far more in leukocytes, contributing greatly to dissecting the molecular mechanisms involved in cell motility toward the tissues and back to vasculature (Holmes et al., 2012; Huttenlocher and Poznansky, 2008; Mirakaj et al., 2011). Also, the negative guidance of the axon growth cone has received significant attention, from the 1990s classical works (Charron and Tessier-Lavigne, 2005; Song et al., 1998; Tessier-Lavigne and Goodman, 1996) up to recent detailed reports on mechanisms of the in vitro (Rajasekharan et al., 2010) and in vivo (Ferrario et al., 2012; Murray et al., 2010) wiring of the nervous system. However, in embryonic cells, particularly NCCs, evidence of chemorepulsion is scarce, with the exception of some works involving the development of the outflow tract of the heart (Toyofuku et al., 2008), and the early migratory NCCs confined to the trunk ventral pathway (Jia et al., 2005). Recent data shows a chemokine system involved in concentration-dependent attraction-repulsion phenomena of NCC-derived melanoma cells, associated with tumoral metastatic expansion (Amatschek et al., 2011). A similar concentration-dependent effect of Shh was depicted on retinal axons (Kolpak et al., 2009). In addition to the present report, recent evidence from our laboratory also shows the bi-phasic concentration effect of the chemokine SDF-1 (Jaurena, 2011), as well as of the morphogen Shh (Tolosa et al., 2012) on cephalic NCCs.

It is important to note that the attraction-repulsion phenomena could be masked by the method of study. Nowadays, a significant proportion of the reports on chemotaxis utilize the less time-consuming variants of Boyden's classic across-filter method

(Boyden, 1962), with which is not possible to determine the proportion of cells migrating opposite to the putative chemotactic molecule (Erlandsson et al., 2004). Among the advantages of real-time dynamic study methods, apart from the detection of repulsive cell migration, is the determination of absolute motility parameters such as cell speed and distance traveled (Rovasio et al., 2012). In this context, the present data indicate that, at a chemoattractive concentration of NT-3 (40 and 80 ng/ml), responsive NCCs do not exhibit variation of cell speed. In contrast, NCC chemoattraction elicited by SCF (Rovasio et al., 2012), or the chemokine SDF-1 (Jaurena, 2011), or the morphogen Shh (Tolosa et al., 2012), was associated with a significantly low cell velocity. This phenomenon was also reported in neurons of the central nervous system attracted by SCF (Erlandsson et al., 2004).

The mechanism of cell repulsion phenomena, as well as the relationship between chemotactic orientation and cell speed, are today still unexplained because the most plausible mechanism leaves a big question whose answer is elusive. In fact, there is still very little consistent evidence for the general notion that similar molecules drive the cell "forward" or "backward", modulating the opposite directional displacements by very small, but significant, changes in some elements of the complex taxis-associated signal chains (Ferrario et al., 2012; Petersen and Cancela, 2000; Song et al., 1998).

As in other regulations, oriented migration depends on complex (yet poorly unknown) signal chains

The canonical TrkC and p75 receptors for NT-3 as well as the TrkA and TrkB were here clearly shown in our NCCs in in vitro and in vivo whole-mount embryo conditions, even though only the specific blocking of TrkB, TrkC and p75 induces a fall in NCC chemotaxis up the NT-3 gradient. Curiously, only TrkB and TrkC, but not the p75 receptor, seem to also participate in the modulation of the distance traveled and cell speed. The functional relationship between different NT-3 receptors on the same cell population is not surprising, as it is known that expression of the p75 receptor inhibits NT-3 signaling by the TrkA receptor (Mischel et al., 2001). Maybe this is why, in our system, the specific blocking of TrkA does not induce inhibition of NCC chemotaxis toward the NT-3 gradient. Our results suggest that TrkB and TrkC together with p75 receptors participate in the NCC orientation mechanism and are required for sensing the gradient of attractant in the extracellular environment. The p75 receptor may also to play a role in defining the speed/distance traveled by the NCCs.

Phosphatidylinositol 3′-kinase (PI3K) has long been known as an important molecule involved in signal chains of the cell migration process, necessary for polarizing the moving cells and their subsequent directional locomotion (Parent and Devreotes, 1999). This important involvement in cell dynamics has led some researchers to regard them as markers for chemotactic migration (Weiner, 2002). In our present experiments, PI3K blocking diminished the NT-3-dependent chemotactic behavior of NCCs, as well as the absolute parameters of distance traveled and cell speed, supporting the essential participation of this molecule in early events of oriented cell motility.

The functional blocking of ERK chain signals also showed the concentration-dependence of the inhibitor on NCC chemotaxis, emphasizing the involvement of this signal chain component on directional cell migration (Coxon et al., 2003). The results of these experiments surprised us since, after 1 μM PD98059 inhibitor treatment, a significant diminution of the proportion of chemotactic responder cells was observed, falling to the control value, but the directional parameter expressed as chemotactic index showed a slight but significant chemotactic behavior of NCCs up the NT-3 gradient. That is to say that, after treatment with 1 μM ERK-inhibitor, a lower number of NCCs responded to the NT-3 gradient, but this cell sub-population was able to migrate with a more directional behavior toward the neurotrophic factor. On the other hand, when the assay was carried out in the presence of 10 μM PD98059, it resulted in chemo-repulsive behavior of NCCs down the NT-3, in both the proportion of migrating cells and the chemotactic index. In the latter condition, the proportion of NCCs migrating up the NT-3 gradient goes down, suggesting that the same cell sub-population experienced a repulsive motion after a hard blockade of the ERK signal chain. This concentration-dependent ERK inhibition may be related, in an unknown way, with the stop signal and/or the by-pass relay mark for the NCC population that must "decide" the arrest of the migration and/or its moving to another final destination. The analysis of the distance traveled and cell speed also showed unexplained significant diminution only when the system NCCs/NT-3 was evaluated in the presence of the lower concentration of ERK inhibitor.

From in vitro to in vivo (whole-mount) embryo developments

The in vitro experiments aim at obtaining data for interpreting the spatiotemporal behavior of cells in vivo, from their emigration at the neural tube cephalic level toward the optic vesicle field. In the chick embryo, mesencephalic NCCs migrate from the neural tube during a temporal window of about 30–35 h of development (Newgreen and Erickson, 1986), and the sub-population of ciliary NCCs orientate toward the optic vesicle region during the following 20 h (Lee et al., 2003). In our in vitro approach, starting with cells obtained from HH 10–11 chick embryos and cultured during 20 h, the mesencephalic NCCs matched the in vivo stage of active migration toward the ocular field, being competent to respond to directional cues as described. In fact, when NT-3 chemotaxis experiments were performed with "older" NCCs coming from 30–40 h of culture time, the guiding property of NT-3 became progressively inefficient, and finally induced a chemo-repulsion effect. These results, together with those showing that NT-3-induced chemotaxis of NCCs started from the first 60 min and was maintained for the 6 h of the experiments, show that in vitro chemotactic behavior may be consistent with that expected for the temporal window of the in vivo condition. In relation to the NT-3 repulsion of "older" NCCs, it may not be too daring to speculate that the bell-shaped behavior suggests that "late arrival" NCCs may be (re-)directed to another "target field".

Supporting this valuable in vitro data, we showed the NT-3 expression of mRNA and protein in the optic vesicle neighborhood of whole-mount chick embryos. The NT-3 location extending toward the region lateral to the mesencephalic level corresponds to the pathway of a subpopulation of NCCs migrating toward the ocular region. It is worth mentioning that, until now, the factor(s) involved in the abrupt directional change of this subpopulation of cephalic NCCs that, after dorsolateral displacement at a mesencephalic level, turns 90° and migrates toward the caudal side of the optic vesicle (Lee et al., 2003), have not been clearly explained. Although the spatiotemporal expression of NT-3 is coherent with the proposed chemotactic guidance for NCCs, these results do not permit inferences about the cell population or the spatiotemporal molecular modulation of the synthesis and secretion of this neurotrophic factor. As expected, the whole-mount embryo immunocytochemistry of NT-3 protein yielded a co-localized mild but constant label, probably because of the extremely weak concentration of chemotactic functional proteins in the extracellular micro-environment. It is known that chemotactic molecules exert their directional effect at a very low concentration, in the nano/pico molar rank (10^{-9}–10^{-12} M) (Mortimer et al., 2008; Teves et al., 2006; Yu et al., 2009).

The optic vesicle localization of NT-3 expression, as well as the corresponding receptor expression in in situ cephalic NCCs, were key facts for the design of decisive whole-mount embryo experiments applying functional blocking approaches. These assays

resulted in a perturbed distribution of cephalic NCCs associated with the experimental blocking of NT-3 or their NCC receptors, supporting our hypothesis about the chemotactic guiding role of NT-3 in this cell population. The significant diminution of NCCs migrating toward the NT-3-morpholino-treated optic vesicle region, or following the inhibition of NT-3 receptors on transfected NCCs, are clearly the result of mistaking the route, and may also explain the more dense NCC population encountered at the mesencephalic level on the same embryonic side. When a source of NT-3 receptor blocker was precisely administered in the vicinity of mesencephalic NCCs, the sub-population normally destined to colonize the optic vesicle field lost its way and arrested its advance toward its natural target site.

As we previously showed that in vitro and in vivo ethanol-exposure induces selective damage in migratory behavior (Rovasio and Battiato, 1995, 2002) and the chemotactic orientation of NCCs (Jaurena, 2011), and that simultaneous NT-3 treatment prevents ethanol-dependent trophic-survival damage (Jaurena et al., 2011), our present data also open stimulating perspectives for the search for preventive and/or therapeutic tools to protect the abnormal cell distribution induced by prenatal ethanol exposure (Rovasio and Battiato, 1995, 2002).

NT-3 is not unique but participates in the chemotactic guidance mechanism of NCCs

As a whole, the present results suggest a general model for in vivo distribution of cephalic NCCs. Early migratory NCCs, confronted with a spatially downward concentration gradient of NT-3 starting at the optic vesicle region, respond with an oriented migration toward their destination field. When in the vicinity of the target gradient source, the higher concentration of the chemotactic factor stops directional guidance, by a receptor saturation mechanism. The factor(s) involved in NT-3 gradient formation/stability are not known, whether a source-sink model, NT-3 consumption by migrating NCCs, or modulation of NT-3 shedding in the source field. The plasticity of canonical/non-canonical NT-3 receptor expression, responding to concentration-dependent functional signals of the ligand, is also unknown and open to fascinating research.

To our knowledge, the present report provides the first direct evidence that NT-3 modifies the directionality of a subpopulation of cephalic NCCs, inducing locomotor behavior typical of chemotactic migratory cells. The fact that not all, but a significant subpopulation of NCCs responds, is a reflection of the molecular heterogeneity of NCCs. Given that NCCs migrate along different pathways and develop various environment-dependent derivatives (Le Douarin and Kalcheim, 1999), it is clear that the identity of the complex receptor-cytoplasmic signal chains of NCCs is not homogeneous, and that not all NCCs are necessarily and simultaneously responsive to the NT-3 (or another) stimulus.

This work supports the proposed chemotactic mechanism after several essential stages: (1st) Choosing a cell population (NCCs) which distributes into defined fields (optic region) of the embryo; (2nd) having direct experimental evidence of directional migration toward a concentration gradient of known molecules (e.g., NT-3); (3rd) showing the expression of this molecule at the domain colonized by NCCs, as well as their receptor(s) in the migrating cell population; (4th) blocking molecules involved in chemotactic behavior/distribution of in vitro/in vivo NCCs (ligand, receptors, signal chain elements); and (5th) evaluating the oriented migration/distribution of the in vitro/in vivo cell population. A similar schedule was applied in cephalic NCCs and different guiding molecules in other works published or in process of publication from our laboratory (Jaurena, 2011; Rovasio et al., 2012; Tolosa, 2013; Tolosa et al., 2012). As a conceptual point, the present results confirm the NT-3 as one of the important guiding molecules for cephalic NCCs, without disregarding other molecules with equivalent (cooperating) functions (Jaurena, 2011; Rovasio et al., 2012; Tolosa et al., 2012).

In conclusion, our in vitro/in vivo approach supports the idea that diffusible guiding factor(s) play a crucial role in embryo ontogenesis, involving chemotactically-oriented NCCs and colonization, induced by a NT-3 concentration gradient emerging from the optic vesicle field as the target site. These data also amplify the functional scope of neurotrophic factors by involving them in new activities as molecular guides for the colonization mechanism of embryonic cells. The findings are also in line with additional cell-guiding activities for chemokines, trophic factors and morphogens, besides their well-known canonical functions.

Acknowledgments

We thank Mr. Joss Heywood for critical reading of the manuscript. Plasmids with gene sequences to produce chNT-3 probes were kindly donated by Dr. F.Hallböök from the Karolinska Institute (Stockholm, Sweden).

This work was supported by the Consejo Nacional de Investigaciones Científicas y Técnicas (CONICET), the Agencia Nacional de Promoción Científica y Tecnológica (FONCYT), the Ministerio de Ciencia y Tecnología de la Provincia de Córdoba and the Secretaria de Ciencia y Tecnología de la Universidad Nacional de Córdoba (Argentina).

Appendix A. Supplementary data

Supplementary data associated with this article can be found, in the online version, at http://dx.doi.org/10.1016/j.ejcb.2013.10.006.

References

Alto, L.T., Havton, L.A., Conner, J.M., Hollis, E.R., Blesch, A., Tuszynski, M.H., 2009. Chemotropic guidance facilitates axonal regeneration and synapse formation after spinal cord injury. Nat. Neurosci. 12, 1106–1115.

Amatschek, S., Lucas, R., Eger, A., Pflueger, M., Hundsberger, H., Knoll, C., Grosse-Kracht, S., Schuett, W., Koszik, F., Maurer, D., Wiesner, C., 2011. CXCL9 induces chemotaxis, chemorepulsion and endothelial barrier disruption through CXCR3-mediated activation of melanoma cells. Br. J. Cancer 104, 469–479.

Barnes, D., Sato, G., 1980. Methods for growth of culture cell in serum-free medium. Anal. Biochem. 102, 255–270.

Battiato, N.L., Paglini, M.G., Salvarezza, S.B., Rovasio, R.A., 1996. Method for treatment and processing of whole chick embryos for autoradiography, immuno-cytochemistry and other techniques. Biotech. Histochem. 71, 286–288.

Belmadani, A., Tran, P.B., Ren, D., Assimacopoulos, S., Grove, E.A., Miller, R.J., 2005. The chemokine stromal cell-derived factor-1 regulates the migration of sensory neuron progenitors. J. Neurosci. 25, 3995–4003.

Bernd, P., 2008. The role of neurotrophins during early development. Gene Expr. 14, 241–250.

Boyden, S.V., 1962. The chemotactic effect of mixtures of antibody and antigen on polymorphonuclear leukocytes. J. Exp. Med. 115, 453–466.

Bradford, M.M., 1976. A rapid and sensitive method for the quantitation of microgram quantities of protein utilizing the principle of protein-dye binding. Anal. Biochem. 72, 248–254.

Breau, M.A., Wilson, D., Wilkinson, D.G., Xu, D.G., 2012. Chemokine and Fgf signaling act as opposing guidance cues in formation of the lateral line primordium. Development 139, 2246–2253.

Carmona-Fontaine, C., Matthews, H.K., Kuriyama, S., Moreno, M., Dunn, G.A., Parsons, M., Stern, C.D., Mayor, R., 2008. Contact inhibition of locomotion in vivo controls neural crest directional migration. Nature 456, 957–961.

Chalazonitis, A., 2004. Neurotrophin-3 in the development of the enteric nervous system. Prog. Brain Res. 146, 243–263.

Charron, F., Tessier-Lavigne, M., 2005. Novel brain wiring functions for classical morphogens: a role as graded positional cues in axon guidance. Development 132, 2251–2262.

Chen, K.C., Ford, R.M., Cummings, P.T., 2003. Cell balance equation for chemotactic bacteria with a biphasic tumbling frequency. J. Math. Biol. 47, 518–546.

Chesini, E., Bigliani, J.C., Zanin, J.P., Rovasio, R.A., Taborda, R.A.M., 2011. Electroporator applying to research on molecular and developmental biology. In: XVIII Congress of Bioingeneering. SABI, Buenos Aires, Argentina, pp. 1–8.

Coxon, P.Y., Rane, M.J., Uriarte, S., Powell, D.W., Singh, S., Butt, W., Chen, Q., McLeish, K.R., 2003. MAPK-activated protein kinase-2 participates in p38

MAPK-dependent and ERK-dependent functions in human neutrophils. Cell Signal. 15, 993–1001.
Del Barrio, M.G., Nieto, M.A., 2002. Overexpression of Snail family members highlights their ability to promote chick neural crest formation. Development 129, 1583–1593.
Del Barrio, M.G., Nieto, M.A., 2004. Relative expression of Slug, RhoB, and HNK-1 in the cranial neural crest of the early chicken embryo. Dev. Dyn. 229, 136–139.
Erlandsson, A., Larsson, J., Forsberg-Nilsson, K., 2004. Stem cell factor is a chemoattractant and a survival factor for CNS stem cells. Exp. Cell Res. 301, 201–210.
Fabro, G., Rovasio, R.A., Civalero, S., Frenkel, A., Caplan, R., Eisenbach, M., Giojalas, L.C., 2002. Chemotaxis of capacitated rabbit spermatozoa to follicular fluid revealed by a novel directionality-based assay. Biol. Reprod. 67, 1565–1571.
Ferrario, J.E., Baskaran, P., Clark, C., Hendry, A., Lerner, O., Hintze, M., Allen, J., Chilton, J.K., Guthrie, S., 2012. Axon guidance in the developing ocular motor system and Duane retraction syndrome depends on Semaphorin signaling via alpha2-chimaerin. Proc. Natl. Acad. Sci. U. S. A. 109, 14669–14674.
Gilbert, S.F., 2003. Developmental Biology, 7th edition. Sinauer Associates, Inc., Sunderland, MA.
Giojalas, L.C., Rovasio, R.A., 1998. Mouse spermatozoa modify their motility parameters and chemotactic response to factors from the oocyte microenvironment. Int. J. Androl. 21, 201–206.
Gómez-Moutón, C., Lacalle, R.A., Mira, E., Jiménez-Baranda, S., Barber, D.F., Carrera, A.C., Martínez, A.C., Manes, S., 2004. Dynamic redistribution of raft domains as an organizing platform for signaling during cell chemotaxis. J. Cell Biol. 164, 759–768.
Gore, B.B., Wong, K.G., Tessier-Lavigne, M., 2008. Stem cell factor functions as an outgrowth-promoting factor to enable axon exit from the midline intermediate target. Neuron 57, 501–510.
Guidobaldi, H.A., Teves, M.E., Uñates, D.R., Anastasía, A., Giojalas, L.C., 2008. Progesterone from the cumulus cells is the sperm chemoattractant secreted by the rabbit oocyte cumulus complex. PLoS ONE 3 (8), e3040, http://dx.doi.org/10.1371/journal.pone.0003040.
Guidobaldi, H.A., Teves, M.E., Uñates, D.R., Giojalas, L.C., 2012. Sperm transport and retention at the fertilization site is orchestrated by a chemical guidance and oviduct movement. Reproduction 143, 587–596.
Hallbook, F., Ibañez, C.F., Ebendal, T., Persson, H., 1993. Cellular localization of brain-derived neurotrofic factor and neurotrophin-3 mRNA expression in the early chicken embryo. Eur. J. Neurosci. 5, 1–14.
Hamburger, V., Hamilton, H., 1951. A series of normal stages in the development of the chick embryo. J. Morphol. 88, 49–82.
Hammerle, B., Tejedor, F.J., 2007. A novel function of DELTA-NOTCH signalling mediates the transition from proliferation to neurogenesis in neural progenitor cells. PLoS ONE 2 (11), e1169, http://dx.doi.org/10.1371/journal.pone.0001169.
Holmes, G.R., Anderson, S.R., Dixon, G., Robertson, A.L., Reyes-Aldasoro, C.C., Billings, S.A., Renshaw, S.A., Kadirkamanathan, V., 2012. Repelled from the wound, or randomly dispersed? Reverse migration behaviour of neutrophils characterized by dynamic modeling. J. R. Soc. Interface 9, 3229–3239.
Huttenlocher, A., Poznansky, M.C., 2008. Reverse leukocyte migration can be attractive or repulsive. Trends Cell Biol. 18, 298–306.
Jaurena, M.B., 78 pp. 2011. The chemokine Stromal cell-Derived Factor-1 participate in the oriented migration of neural crest cells in normal ontogenesis and exposed to ethanol. Biology Sciences School, National University of Cordoba, Argentina (PhD thesis dissertation).
Jaurena, M.B., Carri, N.G., Battiato, N.L., Rovasio, R.A., 2011. Trophic and proliferative perturbations of in vivo/in vitro cephalic neural crest cells after ethanol exposure are prevented by Neurotrophin 3. Neurotoxicol. Teratol. 33, 422–430.
Jia, L., Cheng, L., Raper, J., 2005. Slit/Robo signaling is necessary to confine early neural crest cells to the ventral migratory pathway in the trunk. Dev. Biol. 282, 411–421.
Kasemeier-Kulesa, J.C., McLennan, R., Romine, M.H., Kulesa, P.M., Lefcort, F., 2010. CXCR4 controls ventral migration of sympathetic precursor cells. J. Neurosci. 30, 13078–13088.
Kee, Y., Hwang, B.J., Sternberg, P.W., Bronner-Fraser, M., 2007. Evolutionary conservation of cell migration genes: from nematode neurons to vertebrate neural crest. Genes Dev. 21, 391–396.
Kolpak, A.L., Jiang, J., Guo, D., Standley, C., Bellve, K., Fogarty, K., Bao, Z.Z., 2009. Negative guidance factor-induced macropinocytosis in the growth cone plays a critical role in repulsive axon turning. J. Neurosci. 29, 10488–10498.
Krispin, S., Nitzan, E., Kassem, Y., Kalcheim, C., 2010. Evidence for a dynamic spatiotemporal fate map and early fate restrictions of premigratory avian neural crest. Development 137, 585–595.
Kubota, Y., Ito, K., 2000. Chemotactic migration of mesencephalic neural crest cells in the mouse. Dev. Dyn. 217, 170–179.
Kulesa, P.M., Bailey, C.M., Kasemeier-Kulesa, J.C., McLennan, R., 2010. Cranial neural crest migration: new rules for an old road. Dev. Biol. 344, 543–554.
Laemmli, U.K., 1970. Cleavage of structural proteins during the assembly of the head of bacteriophage T4. Nature 227, 680–685.
Le Douarin, N.M., Kalcheim, C., 1999. The Neural Crest, 2nd edition. Cambridge Univ. Press, Cambridge, UK.
Lee, V.M., Sechrist, J.W., Luetolf, S., Bronner-Fraser, M., 2003. Both neural crest and placode contribute to the ciliary ganglion and oculomotor nerve. Dev. Biol. 263, 176–190.
Lock, J.G., Wehrle-Haller, B., Stromblad, S., 2008. Cell–matrix adhesion complexes: master control machinery of cell migration. Semin. Cancer Biol. 18, 65–76.
Matthews, H.K., Marchant, L., Carmona-Fontaine, C., Kuriyama, S., Larraín, J., Holt, M.R., Parsons, M., Mayor, R., 2008. Directional migration of neural crest cells in vivo is regulated by Syndecan-4/Rac1 and non-canonical Wnt signaling/RhoA. Development 135, 1771–1780.
Mayor, R., Theveneau, E., 2013. The neural crest. Development 140, 2247–2251.
McLennan, R., Dyson, L., Prather, K.W., Morrison, J.A., Baker, R.B., Maini, P.K., Kulesa, P.M., 2012. Multiscale mechanisms of cell migration during development: theory and experiment. Development 139, 2935–2944.
Mirakaj, V., Brown, S., Laucher, S., Steinl, C., Klein, G., Köhler, A., Skutella, T., Meisele, C., Brommer, B., Rosenberger, P., Schwab, J.M., 2011. Repulsive guidance molecule-A (RGM-A) inhibits leukocyte migration and mitigates inflammation. Proc. Natl. Acad. Sci. U. S. A. 108, 6555–6560.
Mischel, P.S., Smith, S.G., Vining, E.R., Valletta, J.S., Mobley, W.C., Reichardt, L.F., 2001. The extracellular domain of p75NTR is necessary to inhibit neurotrophin-3 signaling through TrkA. J. Biol. Chem. 276, 11294–11301.
Molyneaux, K., Wylie, C., 2004. Primordial germ cell migration. Int. J. Dev. Biol. 48, 537–544.
Mortimer, D., Fothergill, T., Pujic, Z., Richards, L.J., Goodhill, G.J., 2008. Growth cone chemotaxis. Trends Neurosci. 31, 90–98.
Murray, A., Naeem, A., Barnes, S.H., Drescher, U., Guthrie, S., 2010. Slit and Netrin-1 guide cranial motor axon pathfinding via Rho-kinase, myosin light chain kinase and myosin II. Neural Dev. 5, 16, http://dx.doi.org/10.1186/1749-8104-5-16.
Nakamura, H., Katahira, T., Sato, T., Watanabe, Y., Funahashi, J., 2004. Gain- and loss-of-function in chick embryos by electroporation. Mech. Dev. 121, 1137–1143.
Natarajan, D., Marcos-Gutierrez, C., Pachnis, V., de Graaff, E., 2002. Requirement of signalling by receptor tyrosine kinase RET for the directed migration of enteric nervous system progenitor cells during mammalian embryogenesis. Development 129, 5151–5160.
Newgreen, D.F., Erickson, C.A., 1986. The migration of neural crest cells. Int. Rev. Cytol. 103, 89–145.
Paratcha, G., Ibañez, C.F., Ledda, F., 2006. GDNF is a chemoattractant factor for neuronal precursor cells in the rostral migratory stream. Mol. Cell. Neurosci. 31, 505–514.
Parent, C.A., Devreotes, P.N., 1999. A cell's sense of direction. Science 284, 765–770.
Paves, H., Saarma, M., 1997. Neurotrophins as in vitro growth cone guidance molecules for embryonic sensory neurons. Cell Tissue Res. 290, 285–297.
Petersen, O.H., Cancela, J.M., 2000. Attraction or repulsion by local Ca^{2+} signals. Curr. Biol. 10, R311–R314.
Rajasekharan, S., Bin, J.M., Antel, J.P., Kennedy, T.E., 2010. A central role for RhoA during oligocendroglial maturation in the switch from Netrin-1-mediated chemorepulsion to process elaboration. J. Neurochem. 113, 1589–1597.
Ramón, Cajal, S., 1892. La rétine des vertebrés. La Cellule 9, 119–258.
Rezzoug, F., Seelan, R.S., Bhattacherjee, V., Greene, R.M., Pisano, M.M., 2011. Chemokine-mediated migration of mesencephalic neural crest cells. Cytokine 56, 760–768.
Ricardo, S., Lehmann, R., 2009. An ABC transporter controls export of a Drosophila germ cell attractant. Science 13, 943–946.
Rovasio, R.A., Battiato, N.L., 1995. Role of early migratory neural crest cells in developmental anomalies induced by ethanol. Int. J. Dev. Biol. 39, 421–422.
Rovasio, R.A., Battiato, N.L., 2002. Ethanol induces morphological and dynamic changes on in vivo and in vitro neural crest cells. Alcohol. Clin. Exp. Res. 26, 1286–1298.
Rovasio, R.A., Delouvee, A., Yamada, K.M., Timpl, J.P., Thiery, J.P., 1983. Neural crest cell migration: requirements for exogenous fibronectin and high cell density. J. Cell Biol. 96, 462–473.
Rovasio, R.A., Faas, L., Battiato, N.L., 2012. Insights into Stem Cell Factor chemotactic guidance of neural crest cells revealed by a real-time directionality-based assay. Eur. J. Cell Biol. 91, 375–390.
Sambrook, J., Fritsch, E.F., Maniatis, T., 1989. Molecular Cloning – A Laboratory Manual, 2nd edition. Cold Spring Harbor Lab. Press, New York.
Sauka-Spengler, T., Bronner-Fraser, M., 2008. A gene regulatory network orchestrates neural crest formation. Nat. Rev. Mol. Cell Biol. 9, 557–568.
Selleck, M.A.J., 1996. Culture and microsurgical manipulation of the early avian embryo. In: Bronner-Fraser, M. (Ed.), Methods in Cell Biology. Chap. 1, Vol. 51. Academic Press Inc., San Diego, CA, pp. 1–21.
Song, H.J., Ming, G.L., He, Z., Lehmann, M., McKerracher, L., Tessier-Lavigne, M., Poo, M.M., 1998. Conversion of neural growth cone responses from repulsion to attraction by cyclic nucleotides. Science 281, 1515–1518.
Streichan, S.J., Valentin, G., Gilmour, D., Hufnagel, L., 2011. Collective cell migration guided by dynamically maintained gradients. Phys. Biol. 8, 045004, http://dx.doi.org/10.1088/1478-3975/8/4/045004.
Sun, F., Giojalas, L.C., Rovasio, R.A., Tur-Kaspa, I., Sanchez, R., Eisenbach, M., 2003. Lack of species-specificity in mammalian sperm chemotaxis. Dev. Biol. 255, 423–427.
Teddy, J.M., Kulesa, P.M., 2004. In vivo evidence for short- and long-range cell communication in cranial neural crest cells. Development 131, 6141–6151.
Tessier-Lavigne, M., Goodman, C.S., 1996. The molecular biology of axon guidance. Science 274, 1123–1133.
Teves, M.E., Barbano, F., Guidobaldi, H.A., Sanchez, R., Miska, W., Giojalas, L.C., 2006. Progesterone at the picomolar range is a chemoattractant for mammalian spermatozoa. Fertil. Steril. 86, 747–749.
Tolosa, E.J., 2013. Embryonic cell distribution: Involvement of Sonic Hedgehog-Gli signals in the oriented motility of neural crest cells. Biology Sciences School, National University of Cordoba, Argentina, pp. 1–91 (PhD thesis dissertation).
Tolosa, E.J., Jaurena, M.B., Zanin, J.P., Battiato, N.L., Rovasio, R.A., 2012. In situ hybridization of chemotactically bioactive molecules on cultured chick embryo. J. Histotechnol. 35, 114–129.

Tosney, K.W., 2004. Long-distance cue from emerging dermis stimulates neural crest melanoblast migration. Dev. Dyn. 229, 99–108.
Toyofuku, T., Yoshida, J., Sugimoto, T., Yamamoto, M., Makino, N., Takamatsu, H., Takegahara, N., Suto, F., Hori, M., Fujisawa, H., Kumanogoh, A., Kikutani, H., 2008. Repulsive and attractive semaphorins cooperate to direct the navigation of cardiac neural crest cells. Dev. Biol. 321, 251–262.
van Haastert, P.J., Keizer-Gunnink, I., Kortholt, A., 2007. Essential role of PI3-kinase and phospholipase A2 in Dictyostelium discoideum chemotaxis. J. Cell Biol. 177, 809–816.
Vincent, M., Duband, J.L., Thiery, J.P., 1983. A cell surface determinant expressed early on migrating avian neural crest cells. Brain Res. 285, 235–238.
von Philipsborn, A., Bastmeyer, M., 2007. Mechanisms of gradient detection: a comparison of axon pathfinding with eukaryotic cell migration. Int. Rev. Cytol. 263, 1–62.
Wehrle-Haller, B., Meller, M., Weston, J.A., 2001. Analysis of melanocyte precursors in Nf1 mutants reveals that MGF/KIT signaling promotes directed cell migration independent of its function in cell survival. Dev. Biol. 232, 471–483.
Weiner, O.D., 2002. Regulation of cell polarity during eukaryotic chemotaxis: the chemotactic compass. Curr. Opin. Cell Biol. 14, 196–202.
Wolfner, M.F., 2011. Precious essences: female secretions promote sperm storage in Drosophila. PLoS Biol. 9 (11), e1001191, http://dx.doi.org/10.1371/journal.pbio.1001191.
Yamauchi, J., Miyamoto, Y., Tanoue, A., Shooter, E.M., Chan, J.R., 2005. Ras activation of a Rac1 exchange factor Tiam1, mediates neurotrophin-3-induced Schwann cell migration. Proc. Natl. Acad. Sci. U. S. A. 102, 14889–14894.
Young, H.M., Bergner, A.J., Anderson, R.B., Enomoto, H., Milbrandt, J., Newgreen, D.F., Whitington, P.M., 2004. Dynamics of neural crest-derived cell migration in the embryonic mouse gut. Dev. Biol. 270, 455–473.
Yu, S.R., Burkhardt, M., Nowak, M., Ries, J., Petrasek, Z., Scholpp, S., Schwille, P., Brand, M., 2009. Fgf8 morphogen gradient forms by a source-sink mechanism with freely diffusing molecules. Nature 461, 533–537.
Zanin, J.P., 2011. Neurotrophin-3 involvement in the modulation mechanism of directional migration of neural crest cells. Biology Sciences School, National University of Cordoba, Argentina, pp. 1–85 (PhD thesis dissertation).
Zhou, P., Porcionatto, M., Pilapil, M., Chen, Y., Choi, Y., Tolias, K.F., Bikoff, J.B., Hong, E.J., Greenberg, M.E., Segal, R.A., 2007. Polarized signaling endosomes coordinate BDNF induced chemotaxis of cerebellar precursors. Neuron 55, 53–68.